K. BEALL

279-0300
x270

JOHN F. ABEL, JR. • Mining Engineer

310 Lookout View Court, Golden, Colorado 80401 • 279-4901

REVIEW OF PROPOSED
WIPP UNDERGROUND MINE DESIGN

by

John F. Abel, Jr.

Colorado P.E. 5642

November 15, 1979

JOHN F. ABEL, JR. 5642 PROFESSIONAL ENGINEER STATE OF COLORADO

John F. Abel Jr.

SUMMARY

The yield pillar concept presented by Bechtel should be safe for construction of the WIPP facility. The designed yield pillars will indeed yield to shed unsupportable tributary area loads to the adjacent semi-infinite abutments in the case of the entry design. The storage room abutment pillars are far from semi-infinite in width. As such they will be subject to considerable creep shortening. If the yield pillar concept is chosen the size of the abutment pillars should be increased to 400 by 400 ft.

The presence of a 15-ft thick uniform salt roof removes any necessity for a yield pillar design. Conventional room and pillar design has a long and successful history of application in salt mining, including the Carlsbad district. Bechtel's confidence in conventional room and pillar stability has been demonstrated in their shop pillar design.

The 1000-ft radius shaft pillar appears rather conservative. The strength of this pillar is more than sufficient to carry any conceivable load. The subsidence protection offered by the shaft pillar can only be evaluated if the strain tolerance of the surface structures is known.

The design verification test panel is too short to provide a meaningful test of the yield pillars. An increase in test panel length of 100 ft is recommended.

The placement of RH cansiters in horizontal drillholes in the abutment pillars should be accompanied by an increase in abutment pillar size, unless it is intended to retreat from the access drifts at the time of drilling and placement.

TABLE OF CONTENTS

INTRODUCTION

Mine design is an inexact science. The inability to define the geologic environment, to determine the rock mass properties and to define the in situ stress field necessitate design under a high degree of uncertainty. No mine design is ever complete until it is tested in actual practice.

Two words that are generally true of successful mine design are simplicity and flexibility. Room and pillar mining operations are in general simple in concept and simple in execution, and capable of incorporating changes in design once access is possible. A complicated design, such as the use of panel (abutment) and yield pillars is only resorted to when either geologic or stress conditions prevent successful application of conventional room and pillar mining or subsidence protection is necessary for surface structures.

The purpose of this report was to evaluate what is in effect a combined yield pillar and conventional room and rigid pillar design. The yield pillar design method was used for entries and storage rooms. Conventional rigid pillar design was used for shop and shaft pillars.

DESIGN PROPERTIES FOR WIPP ROCK SALT

The evaluation of entry and room pillar designs necessitates the estimation of the rock mass physical properties of the rock salt. Data on specimen compression strength is presented in GRC Chapter 9 in Tables 9.2.4.-1 and 9.2.4.-2. On page 9-14 the angle of internal friction (ϕ) at 2700-ft depth is given approximately 33° and apparent cohesion of 1000 psi. Table 1 presents the data and the calculated best-fit statistical approximations for this data, namely Φ equals 29.6° and cohesion equals 937 psi for all samples test reported. These results are also presented on Figures 1 and 2.

The reasonableness of these values for specimem properties of rock salt and associated evaporites is indicated by comparison of these properties with those obtained from Menzel, Eckart, Bruckner and Thoma (1972, Paper 27, p. 2, 5th Int'l. Strata Control Conf.) and presented on Figures 3 - 6. In fact, the specimen compression strength properties obtained from the GRC Chapter 9 reported properties are slightly lower than those reported by Menzel, et.al.

The application of the confined core pillar design method requires consideration of the decrease in compression strength with increase in size of the specimen tested. Table 2 presents some indications of this decrease in strength with increase in size of specimen tested. Hobbs (1970) demonstrated that the angle of internal friction determined from triaxial testing is constant, irrespective of whether the rock is intact or broken. Figure 7 shows this result. Wilson (1972) suggests that the "failure stress of the pillar edge" which is the unconfined compression strength of large samples "is a measure of the initial cohesion between the grains (zero if the rock is broken)".

I have employed 30° for the angle of internal friction (ϕ) and two values for the pillar edge strength (σ_6); namely 937 psi, the rock specimen cohesion, From GRC Chapter 9, Table 9.2.4-1 and Table 9.2.4-2

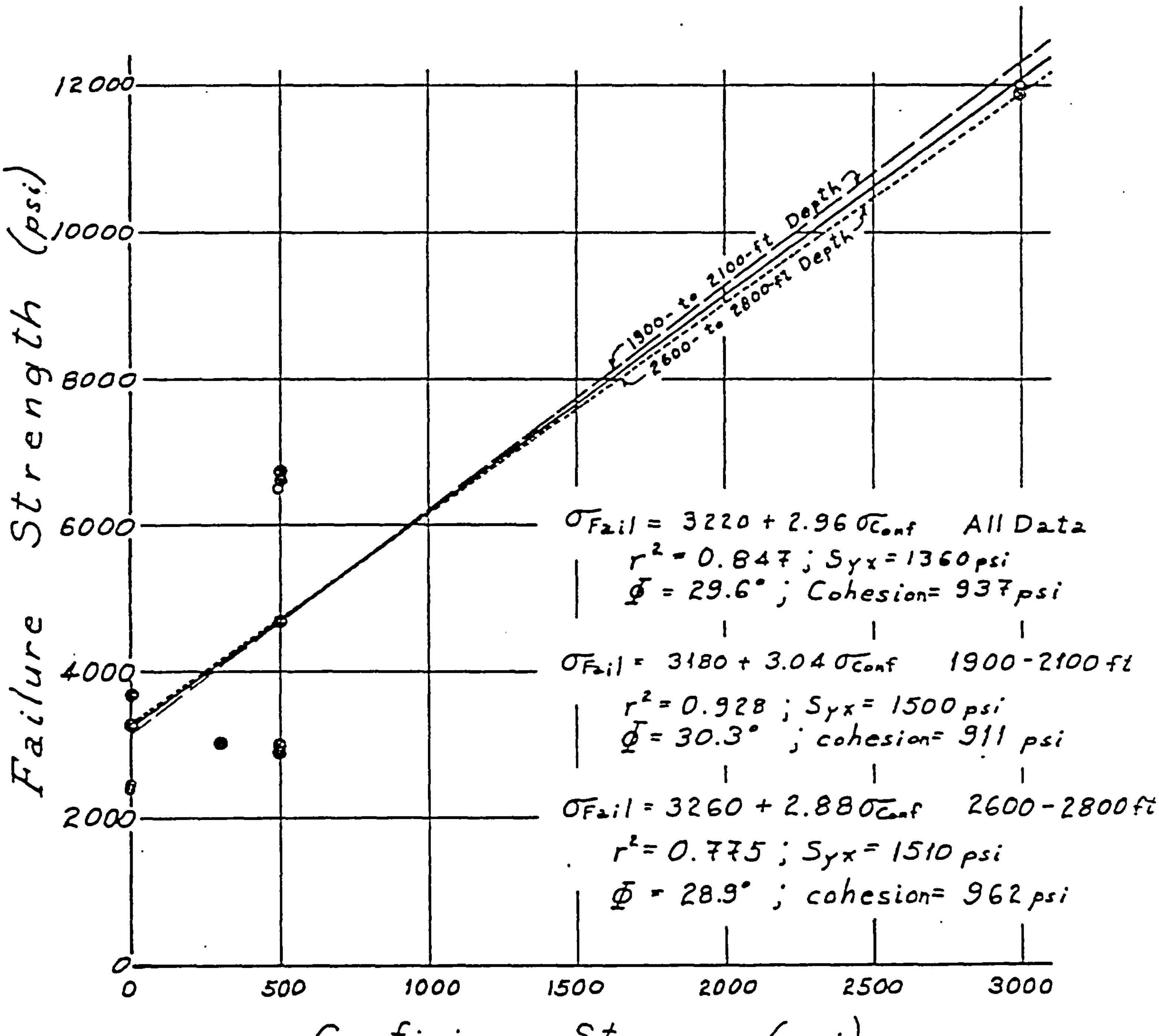

Figure 1. Triaxial test results from boreholes AEC 7 and ERDA 9.

From GRC Chapter 9, Table 9.2.4.-1 and Table 9.2.4.-2, boreholes AEC 7 and ERDA 9

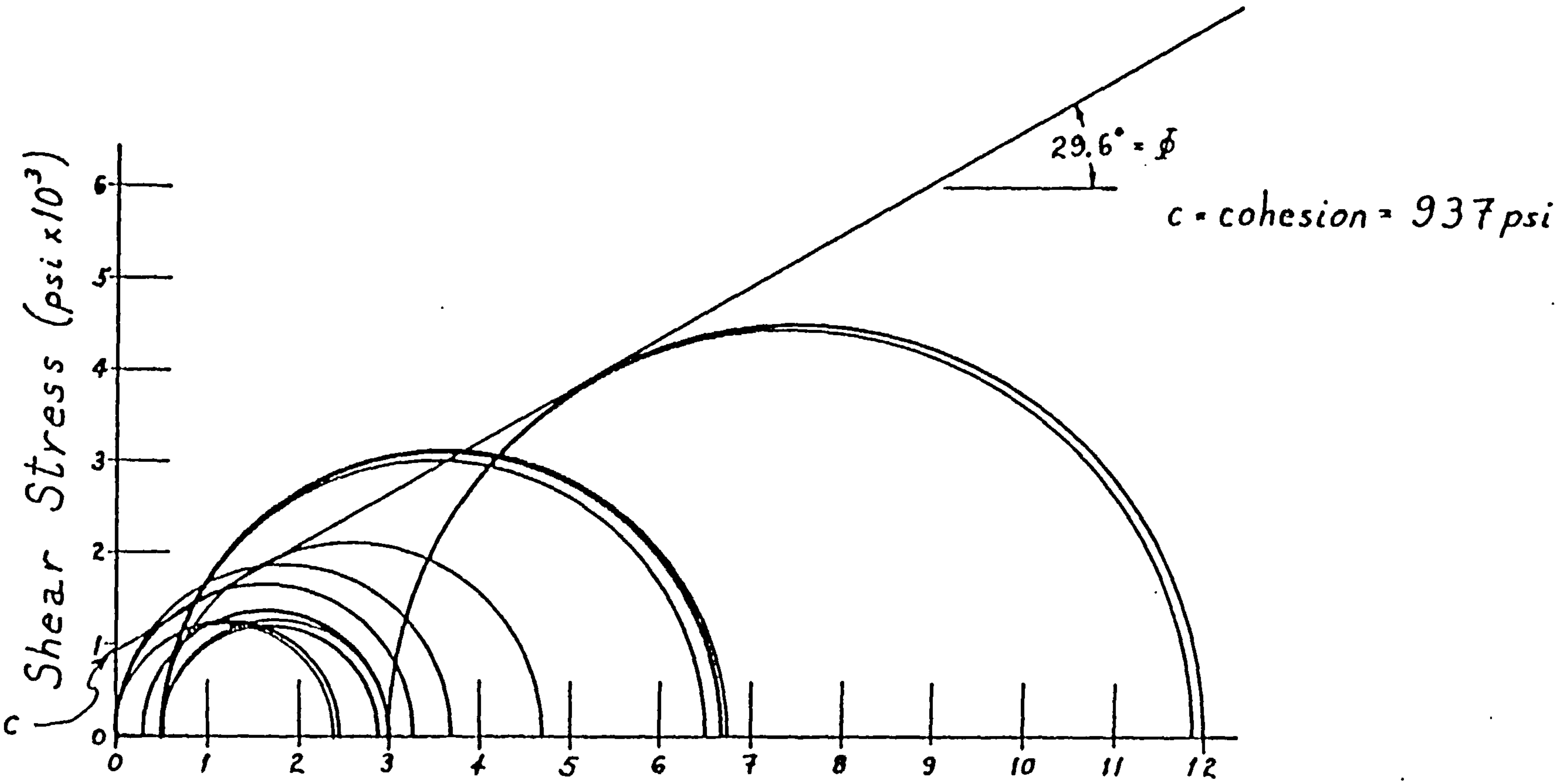

Figure 2. Mohr's envelope at ultimate strength.

TABLE 1

EVALUATION OF TRIAXIAL COMPRESSION TEST RESULTS FOR WIPP STUDY AREA (GRC Chapter 9, Tables 9.2.4.-1 and 9.2.4.-2)

Depth (ft)	Confining Stress(psi)	Failure Stress(psi)
1900	0	2450
2700	0	3700
2100	0	2400
2700	0	3300
2100	500	6500
2100	3000	>12000
2600-2700	500	6800
2600-2700	3000	>11900
2700-2800	500	> 6700
2700-2800	500	≃ 4700
2700-2800	500	≃ 2900
2700-2800	300	> 3050
2600	500	> 3000

ALL DATA

Failure Strength (psi) = 3220 + 2.96 (Confining Stress-psi)

r^2 = 0.847; Syx = 1360 psi; calc = 7.80

ϕ = 29.6°; Cohesion = 937psi

1900-2100-ft DEPTH

Failure Strength (psi) = 3180 + 3.04 (Confining Stress-psi)

r^2 = 0.928; Syx = 1500 psi; calc = 5.06

ϕ = 30.3°; Cohesion = 911psi

2600-2800-ft DEPTH

Failure Strength (psi) = 3260 + 2.88 (Confining Stress-psi)

r^2 = 0.775; Syx = 1510 psi; calc = 4.90

ϕ = 28.9°; Cohesion = 962psi

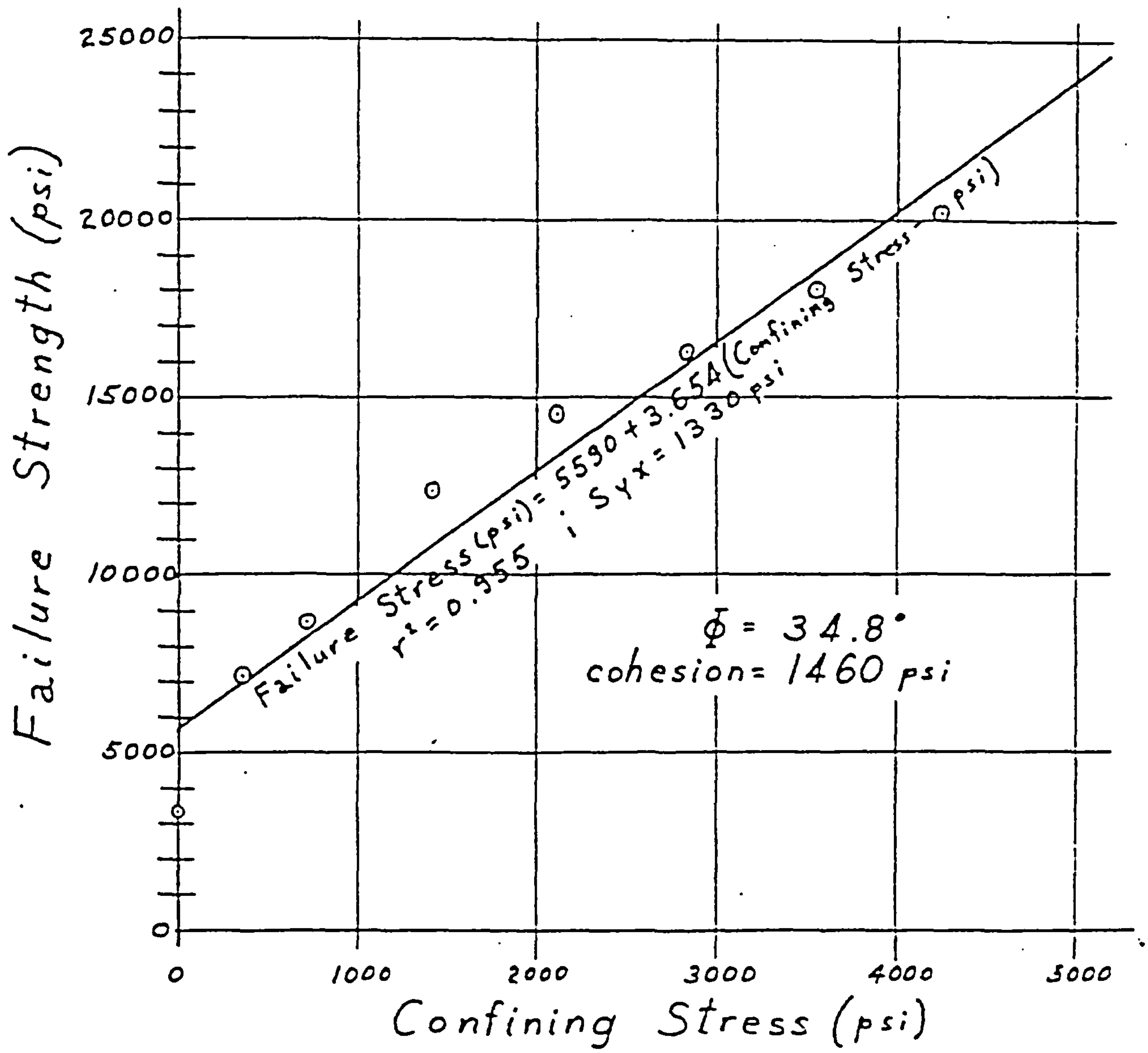

Intact rock salt properties (from Menzel, et. al., 1972, Proc. 5th Int'l. Strata Control Conf.)

Figure 3.

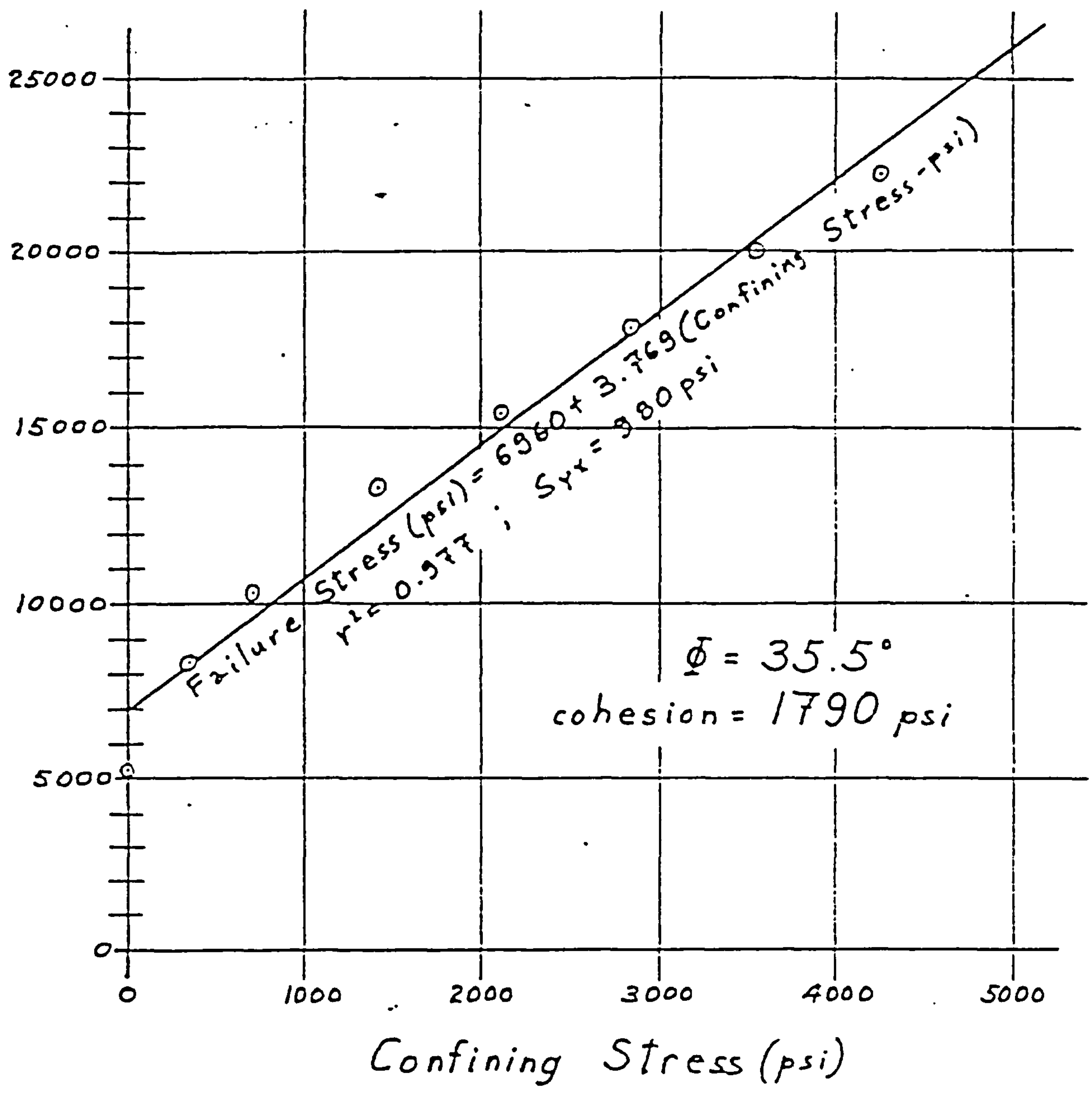

Intact "Hard Salt" (Hartsalz) properties (from Menzel, et. al., 1972, Proc. 5th Int'l. Strata Control Conf.)

Figure 4.

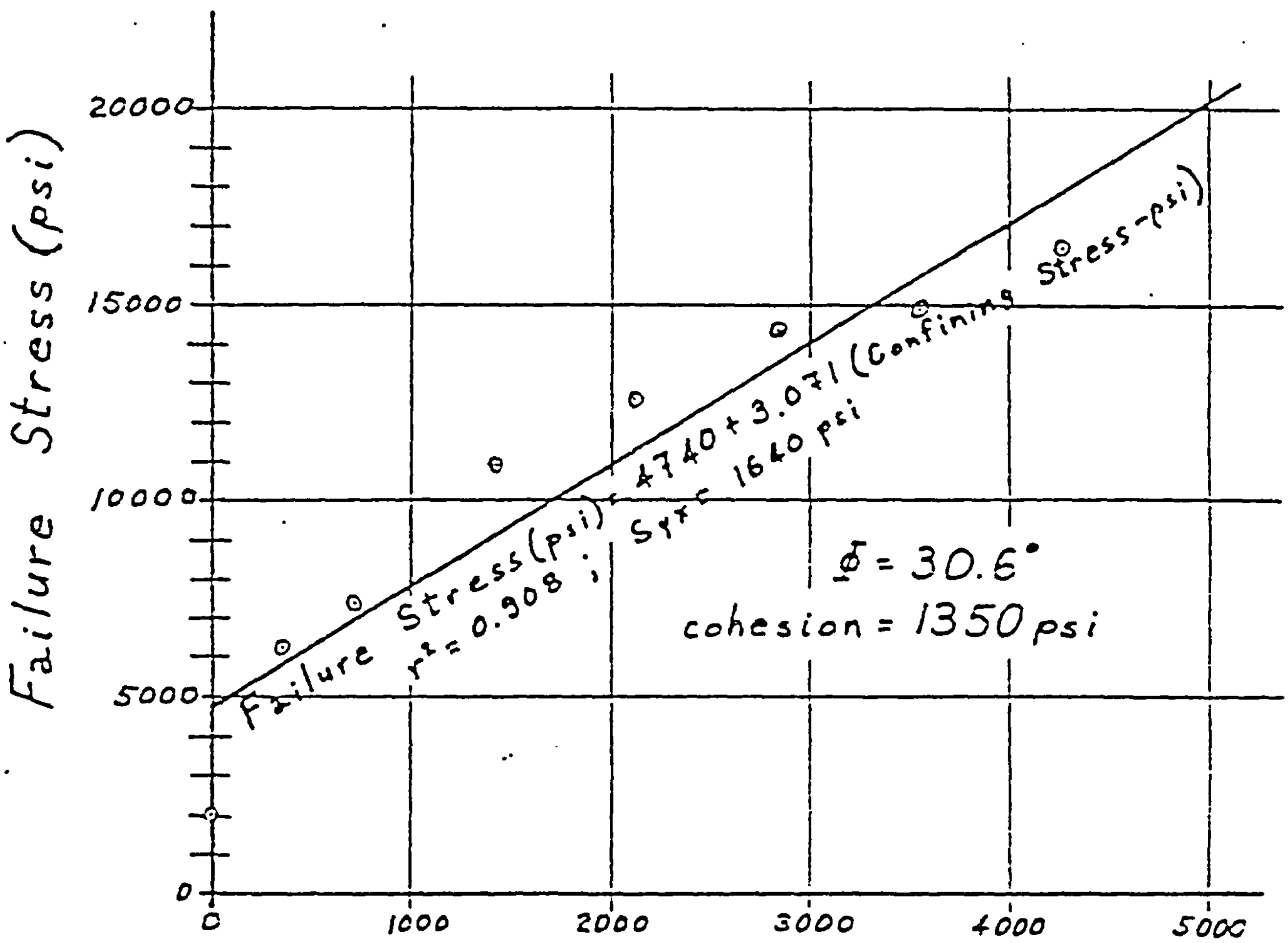

Intact carnolite salt properties (from Menzel, et. al., 1972, Proc. 5th Int'l. Strata Control Conf.)

Figure 5.

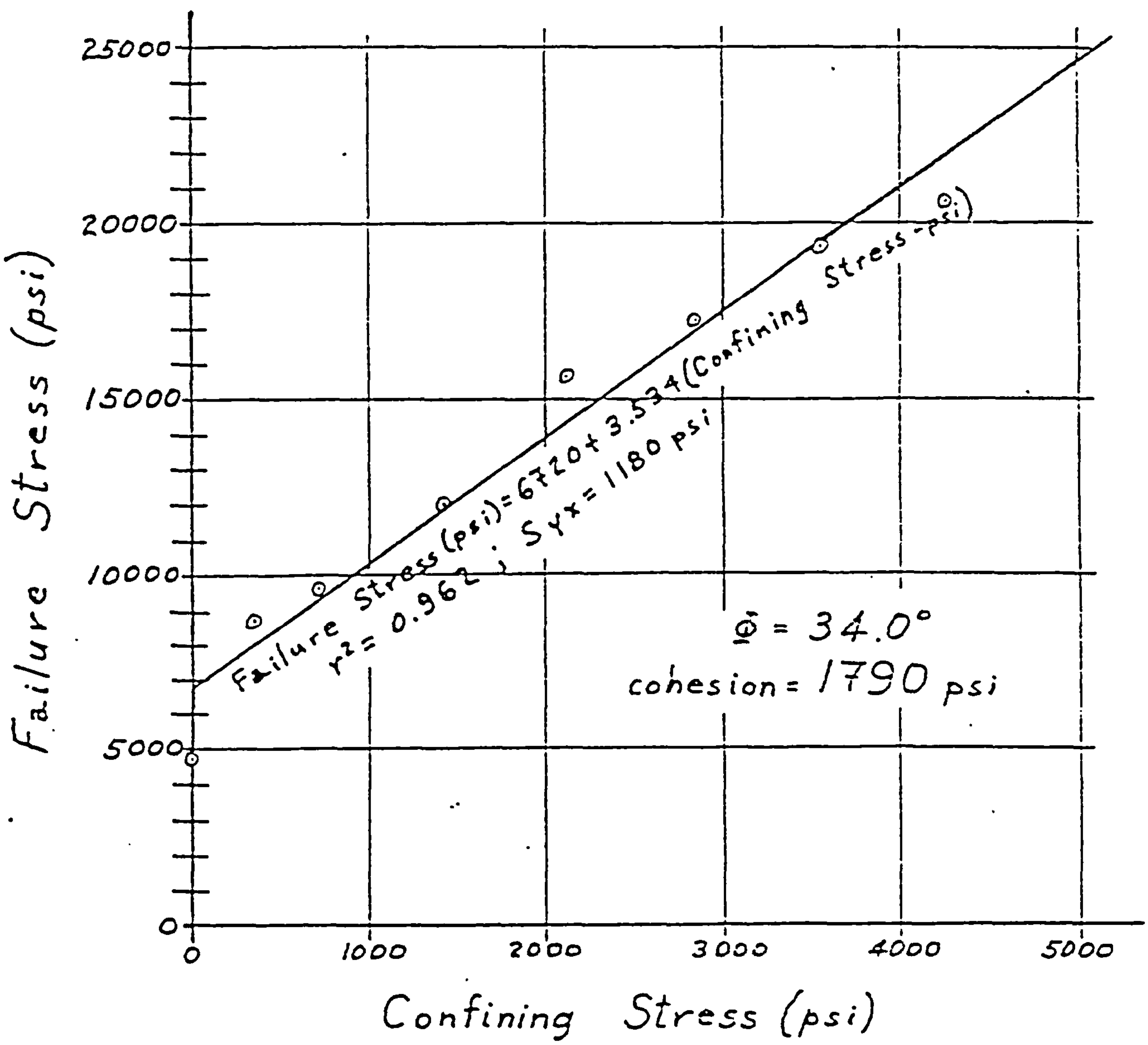

Intact sylvite (Sylvinit) salt properties (from Menzel, et. al., 1972, Proc. 5th Strata Control Conf.)

Figure 6.

TABLE 2. Uniaxial compression strength decrease with increasing specimen size

COAL
(Bieniawski, 1968)

Side Length (in.)	Strength (psi)
0.75	4260
1	4760
2	4880
2.7	4575
3	4070
6	1850
12	1158
18	910
24	800
28	774
36	709
48	650
60	644
Increase 80 times	Decrease 85%

ROCK SALT
(Patrick Harrison, 1963)

Side Length (in.)	Strength (psi)
1.8	4210
2	4000
3.4	3560
4.8	3320
18	1920
Increase 10 times	Decrease 54%

QUARTZ DIORITE
(Pratt and Others, 1972)

Side Length (in.)	Strength (psi)
3.18	4420
4.24	4530
4.5	3860
8	3340
12	1980
18	1400
24	1660
36	1080
72	1330
108	990
Increase 34 times	Decrease 78%

ANHYDRITE
(Skinner, 1956)

Side Length (in.)	Strength (psi)
0.5	32,500
1	25,300
2	24,400
5	16,900
Increase 10 times	Decrease 48%

GRANITE
(Lundberg, 1967)

Side Length (in.)	Strength (psi)
0.75	31,100
1.1	30,100
1.5	25,500
2.3	24,800
Increase 3 times	Decrease 20%

FIGURE 7: Relationship between confining pressure and failure strength (Wilson, 1972, p. 410)

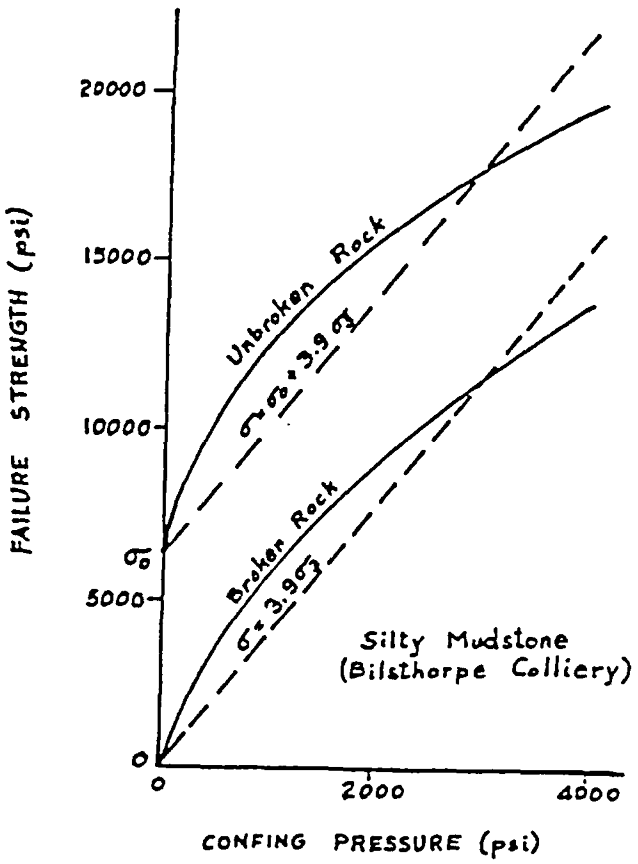

and 450 psi, a more conservative estimate. The 450 psi value of σ_o is based on the specimen compression strength of about 3220 psi reduced about 7 times. This relates to a similar reduction of about 7 times reported by Bieniawski (1968), as shown on Table 2.

The conservatism of assuming that the angle of internal friction (ϕ) is 30^o and the pillar edge strength (σ_o) is 450 psi is indicated by the analysis of room and pillar evaporite mines presented in Table 3. This table was constructed from a review of published data and employed the confined core pillar design method. The indicated factors of safety of less than unity, indicating pillar failure, really indicate the relative conservatism in the selection of the same ϕ and σ_o for all the evaporite formations. Obviously, many of the evaporites are stronger than indicated for the room and pillar configurations.

LOAD TRANSFER DISTANCE ESTIMATION

Yield pillar design as employed in Design #1, or the QUAD room design, necessitates selection a pillar which will yield under tributary area loads (TAL) but which can carry the reduced load after transfer to nearby abutment pillar(s). The estimation of TAL is relatively simple, half the distance to each adjacent pillar and all the rock overhead to the surface.

The estimation of the portion the TAL which will be transfered to the abutment pillar(s) is dependent on the load transfer distance. Table 4 presents data on reported load transfer distances, which is graphically presented on Figure 8. As can be seen, no load transfer distance data is available at depths below 1820 ft. The load transfer distance was extrapolated from the best fit parabola, as follows:

TABLE 3

INDICATED FACTORS OF SAFETY FOR PILLARS IN OPERATING SALT AND POTASH MINES

Mine Identification and Type		Product	Depth (ft)	Pillar Width (ft)	Pillar Length (ft)	Room Height (ft)	Room Width (ft)	Percent Extraction %	Design(1) Strength (psi)	TAL(2) Stress (psi)	Apparent Factor of Safety
1977	Cote Blanche - Dome	Salt	1290	100	100	23	50	56	3000	2720	1.10
1977	Belle Isle - Dome	Salt	1290	40	---(4)	23	60	60	2470	2810	0.88 (3)
1964	Winsford - Bedded	Salt	480	90	90	20	200	90	1500	4800	0.31 (3)
	England			100	100	20	100	75	1530	1800	0.85
1972			580	65	65	20	65	75	1420	2080	0.68
1974	Dravo (1)	Salt	1980	80	130	17	50	56	4600	4180	1.10
	Dravo (2)	Salt	1300	110	110	60	80	66	1910	3640	0.53
	Dravo (3)	Salt	1060	60	60	10.5	65	77	2780	4310	0.64
1971	Headley, Canada - Bedded	Salt	1760	210	210	40	40	40	4060	2730	1.49
				150	150	40	45	41	3600	2790	1.29
1970	Hutchinson - Bedded	Salt	1024	50	---(4)	6	20	71	2750	3360	0.82
				50	50	10	50	75	2620	3840	0.68
				50	50	12	50	75	2490	3840	0.65
				40	40	10	50	80	2460	4860	0.51
1970	Goderich, Canada - Bedded	Salt	1760	200	200	45	65	43	3840	2900	1.33
1974	Dravo (4)	Evapor.	1030	60	60	5.5	32	57	2930	2200	1.33
	Dravo (5)	Evapor.	1570	42	42	10	28	64	2580	2790	0.93
	Dravo (6)	Evapor.	800	25	25	8	25	75	1910	3000	0.63
	Dravo (7)	Evapor.	3140	126	4000	8	67	36	8780	4600	1.91
1965	Barr, Germany - Bedded	Potash	2630	23	820	7.2	11.8	35	5890	3870	1.52
1971	Barr, Canada - Bedded	Potash	3140	54	---(4)	10	20	27	7780	4030	1.93
1973	Esterhazy - Bedded	Potash	3150	90	---(4)	8	61	40	9310	4960	1.73
1958	U.S. Potash - Bedded	Potash	1200	58	58	12.75	32	58	2510	2260	1.11

Notes: (1) Design strength based on $\gamma = 135$ lb/ft^3; $\Phi = 30^\circ$; cohesion = 450 psi & Wilson analysis.
(2) TAL = Tributary area load --- halfway to adjacent pillar, all the way to surface.
(3) Pillar deterioration indicated.
(4) Long rib pillars of unspecified length.

TABLE 4

LOAD TRANSFER DISTANCE DATA

Depth (ft)	Distance (ft)	Depth (ft)	Distance (ft)
350 (1)	50	354 (3)	85
455	90	362	91
360	110	442	100
600	120	448	100
415	130	483	111
600	155	474	115
500	170	541	130
555	180	530	120
730	200	310 (2)	28
875	210	210	9
960	195	270	40
555	225	270	40
710	210	240	30
970	235	365	62
1225	250	365	23
1200	255	405	68
1160	265	300 (4)	90
1015	295	700	165
1455	290	450	128
1575	295	1200	240
1320	320	135 (5)	14.7
1210	325	1100 (6)	350
1415	355	1100	200
1820	410	500 (7)	105

Notes: (1) 7th Progress report of an investigation into the cause of falls and accidents due to falls, Trans. Inst. Min. Engrs.; vol. 108, 1948-49, pp. 489-510.

(2) Alves, C.A., Rock mechanics instrumentation applied to longwall coal mining; Unpublished thesis, Colo. Sch. of Mines, 1977, 224 p.

(3) Stewart, C.L., Rock mass response to longwall mining of a thick coal seam utilizing shields type supports; Unpublished thesis, Colo. Sch. of Mines, 1977, 384 p.

(4) Martin, C.H. and Hargraves, A.J., Shortwall mining with power supports in the Broken Hill Pty. Co. Ltd. mines in Australia; <u>in</u> 5th Int'l. Strata Control Conf., 1972, Paper 13, 13 p.

(5) Briggs, H. and Ferguson, W., Investigation of mining subsidence at Barbauchlaw Mine, West Lothian; Trans. Inst. Min. Engrs. vol. 85, 1932-33, pp. 303-334.

TABLE 4 (Continued)

LOAD TRANSFER DISTANCE DATA

Notes: (6) Frost, L. and Zorychta, H., Rapid development of longwall retreating in the submarine area of the Sydney Coalfield of Nova Scotia; in Proc. Int'l. Conf. on Rapid Excavation in Coal Mines, INCHAR, Liege (BELGIUM), 1963, Paper C9, 13 p.

(7) Parrish, C., Personal communication on J.J. # 1 Mine, Sohio Natural Resources Co., 1979.

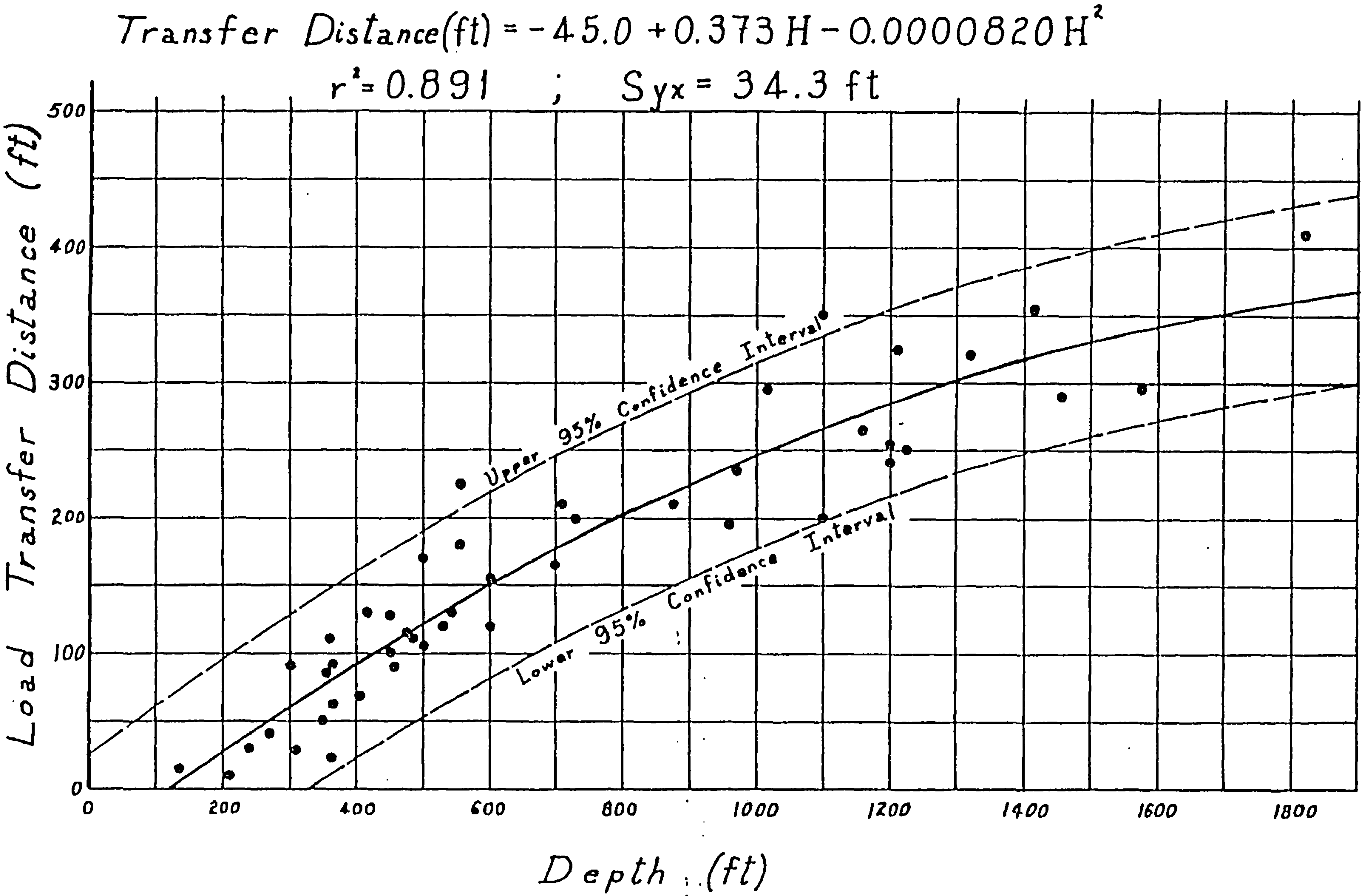

Figure 8.

Oct. 21, '79

Transfer Distance

at 1700-ft = 352.120 ft

at 1800-ft = 360.720 ft

Difference = 8.600 ft

$$\frac{2138 - 1800}{100} = 3.38$$

$$3.38\ (8.600) = 29.068 \text{ ft}$$

$$+\ 360.720 = \underline{\underline{389.788 \text{ ft}}}$$

Load transfer distance estimate at 2138-ft depth

YIELDED PILLAR LOAD ESTIMATION

If a pillar is unable to carry the tributary area load (TAL) as a rigid pillar it will be forced to yield. The load which it must carry after yielding is that portion of the TAL which cannot be transfered to the nearby abutment pillar(s). T. R. Seldendrath (1954, p. 46) suggested using an ellipse as a theoretical approximation of the arch. Steart (1954, p. 311) recommended using a parabola to approximate the load transfer arch shape. A parabolic arch has been employed to calculate the height of rock above a yielding, or TAL overloaded, pillar that cannot be transfered to nearby abutment pillars. It seems illogical to assume the transfer capability should be less effective at the edge of the abutment than further from the abutment as would be the case for the ellipse.

The horizontal limit for the parabola is the load transfer distance, 390 ft in the case of 2138 ft of depth. In other words pillars more than 390 ft from an abutment pillar must carry the full TAL. A pillar less than 390 ft from an abutment pillar can shed the rock above the parabolic arch by yielding. The yielded pillar must carry the column of rock overhead beneath the parabolic arch and halfway to the adjacent pillars.

The following example should clarify the method:

GIVEN: Depth (H) = 2138 ft; Load transfer distance (AD) - 390 ft
Distance to abutment (ℓ) - 80 ft

CALCULATE: Arch height (d)

$$d = \frac{H}{4AD^2}\left(8\ AD\ell - 4\ell^2\right)$$

$$d = \frac{2138}{4(390)^2}\left[8\ (390)\ 80 - 4\ (80)^2\right] = \underline{787\ \text{ft}}$$

This describes one side of the entry pillars in the yield pillar design (Design #1). However, even at a depth of 787 ft load can be transfered to the other abutment, 80 ft away, as follows.

$$AD = 45.0 + 0.373\ (787) - 0.0000820\ (787)^2 = 198\ \text{ft}$$

$$d = \frac{787}{4(198)^2}\left[8\ (198)\ 80 - 4\ (80)^2\right] = \underline{508\ \text{ft}}$$

Figure 9 presents the predicted rock arch over the entry yield pillars which must be carried by the entry pillars after they have yielded.

EVALUATION OF ROOM AND PILLAR SIZES

The traditional applications of yield pillar design has been either to maximize extraction or to reduce subsidence effects at the surface. Yield pillars have also been used to prolong the life of entries in deep evaporite mines.

The transfer of load to adjacent abutment pillars shields yielded pillars from TAL loads and, therefore, slows the shortening of entry pillars. Figure 9

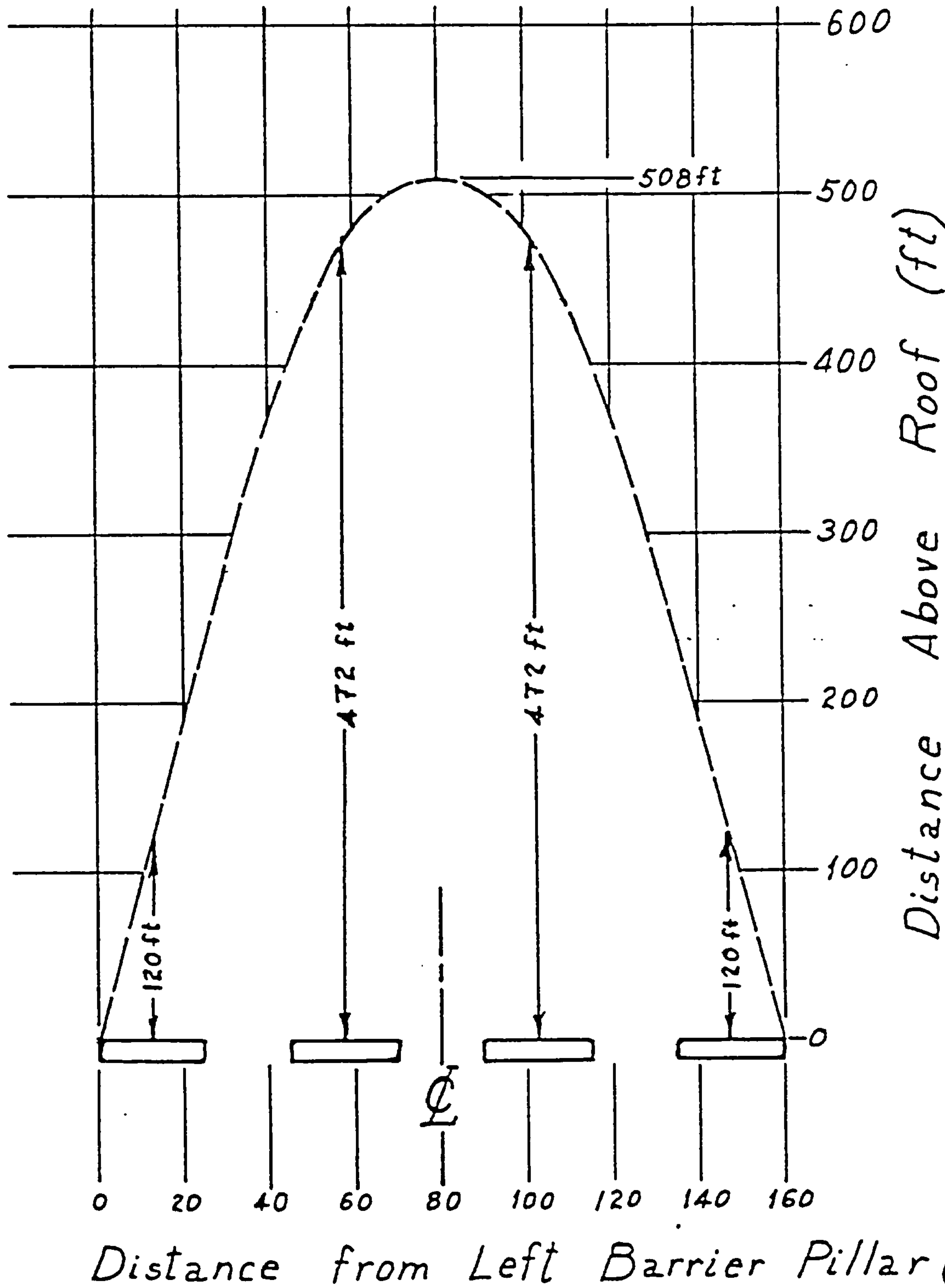

Predicted arch load on entry yield pillars.

Figure 9.

presents the estimated rock load after yielding of the entry yield pillars in Design #1. The data is presented in Table 5. The entry pillars lack the strength to function as rigid pillars. In fact, the entry pillars are so shielded by the nearby abutment pillars that the pillar shortening predicted using Lomenick's creep equation is less than ½ in. after 50 years. This is shown in Figure 10. The temperature employed was 27^{o} C.

The yield pillar design for storage rooms (Design #1 - QUAD Rooms) differs from the entry yield pillar design because of the adjacent abutment pillars. In the case of the entry design the abutment pillars are effectively infinite, i.e. greater in width than in load transfer distance. The 300-ft wide abutment pillars adjacent to the storage rooms should be subject to additional loading over their entire area as the result of the yielding of the room pillars. The width of a pillar would have to equal or exceed the load transfer distance if one side of a pillar is not to be affected by excavation at the opposite side of the pillar. At the WIPP horizon the indicated mean abutment pillar width is 390 ft and the upper 95% confidence limit width is 460 ft.

The yield pillar evaluation for the Design #1 (QUAD) storage rooms is persented in Table 6. The room pillars appear to be incapable of supporting tributary area loads and yielding is predicted, irrespective of the pillar edge strength ($\sigma_{\overline{o}}$) employed. When the pillars between QUAD rooms yield the majority of the room pillar loads will be shed to the abutment pillars, as indicated on Table 6 and Figure 11.

The abutment pillars in the central part of the storage area will be loaded from the yielding storage room pillars on both sides. Since these abutment pillars are less than a load transfer distance in width they will

TABLE 5

STABILITY OF 20- BY 300-FT ENTRY PILLARS
(Design #1 - QUAD Entries)

Pillar	Strength $\phi = 30^0$; $\sigma_o = 450$psi (Tons x 10^6)	Rigid Pillar Load (Tons x 10^6)	Factor of Safety	Yielded Pillar Load (Tons x 10^6)	Factor of Safety
Central	1.50	2.24	0.67	0.52	2.89
Outside	1.50	2.24	0.67	0.34	4.48
	$\phi = 30^0$; $\sigma_o = 937$psi				
Central	1.97	2.24	0.88	0.52	3.78
Outside	1.97	2.24	0.88	0.34	5.86

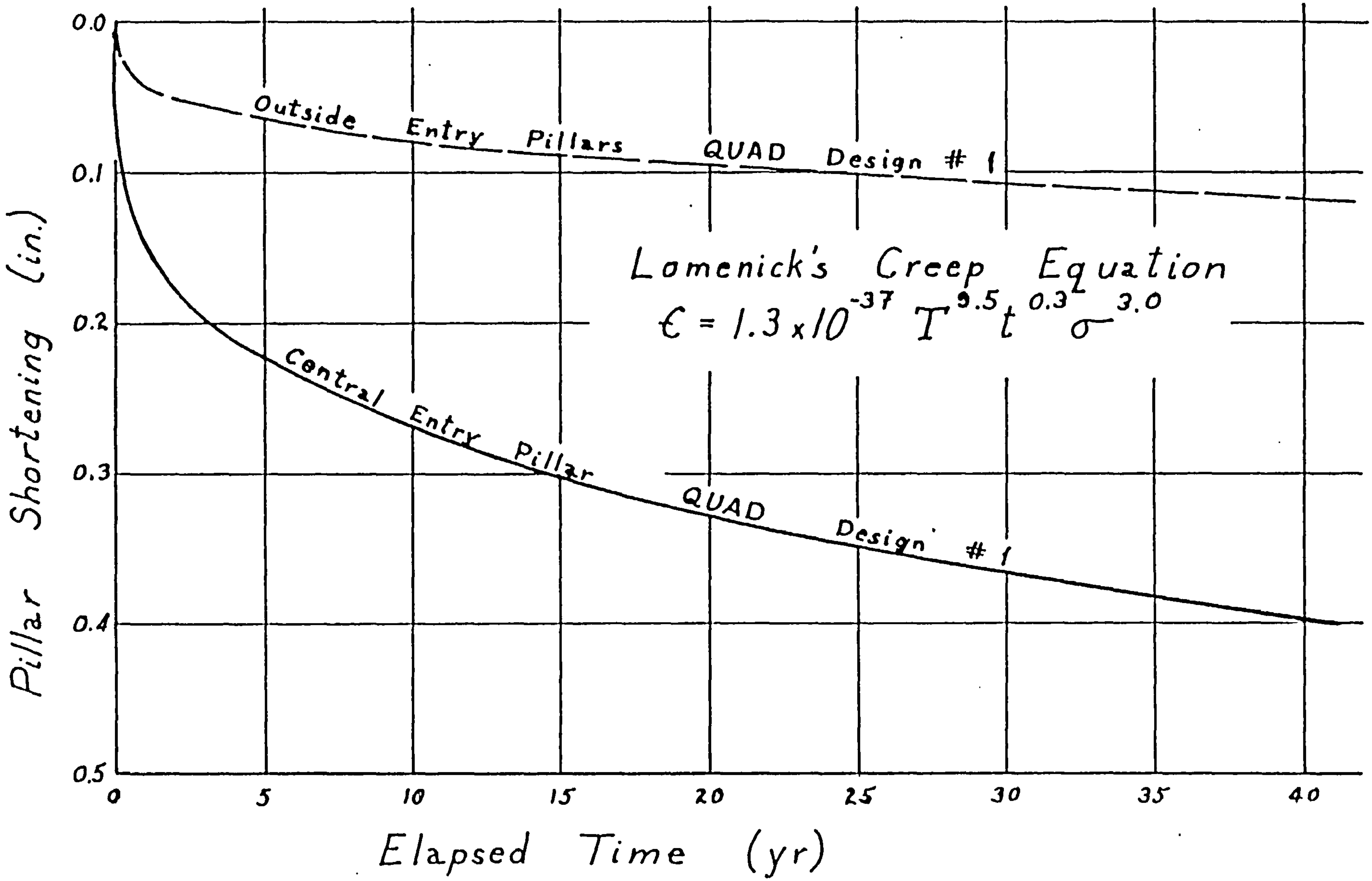

Outside Entry Pillars QUAD Design # 1
Lomenick's Creep Equation
$\epsilon = 1.3 \times 10^{-37} T^{9.5} t^{0.3} \sigma^{3.0}$
Central Entry Pillar QUAD Design # 1
Pillar Shortening (in.)
0.0
0.1
0.2
0.3
0.4
0.5
0
5
10
15
20
25
30
35
40
Elapsed Time (yr)

Figure 10a.

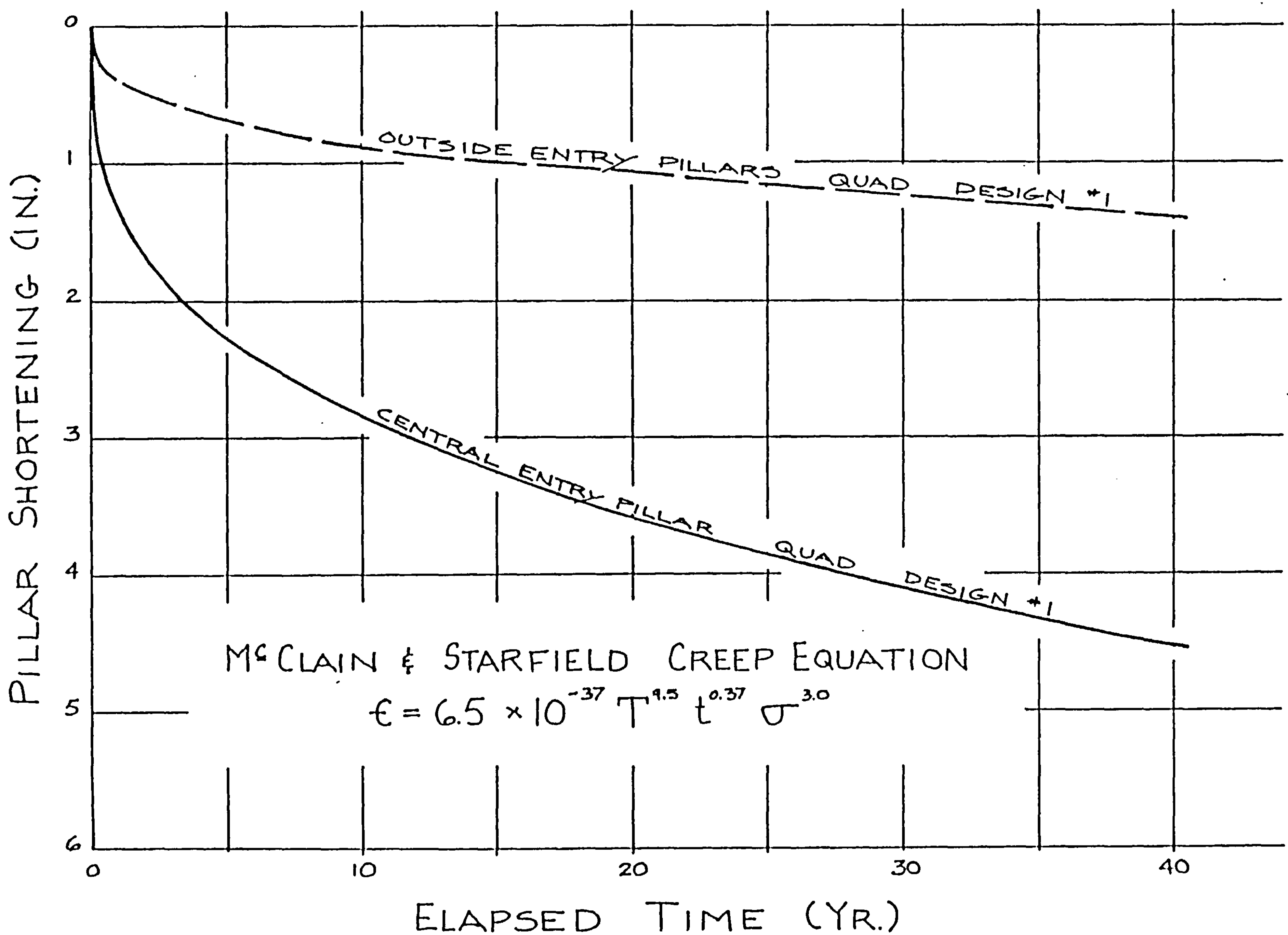
PILLAR SHORTENING (IN.)
0
1
2
3
4
5
6
ELAPSED TIME (YR.)
0
10
20
30
40
OUTSIDE ENTRY PILLARS QUAD DESIGN #1
CENTRAL ENTRY PILLAR QUAD DESIGN #1
McCLAIN & STARFIELD CREEP EQUATION
$\epsilon = 6.5 \times 10^{-37} T^{9.5} t^{0.37} \sigma^{3.0}$

Figure 10b.

TABLE 6

STABILITY OF ROOM PILLARS FOR YIELD PILLAR DESIGN
(Design #1-QUAD Rooms)

Pillar	Strength $\phi = 30^0; \sigma_o = 450$psi (Tons x 10^6)	Rigid Pillar Load (Tons x 10^6)	Factor of Safety	Yielded Pillar Load (Tons x 10^6)	Factor of Safety
Central 25- by 300-ft	2.09	2.89	0.72	0.87	2.40
Outside 25- by 300-ft	2.09	2.89	0.72	0.57	3.66
Abutment 300- by 300-ft	40.46	16.60	2.44	23.26	1.74
	$\phi = 30^0; \sigma_o = 937$psi				
Central 25- by 300-ft	2.63	2.89	0.91	0.87	3.02
Outside 25- by 300-ft	2.63	2.89	0.91	0.57	4.61
Abutment 300- by 300-ft	44.15	16.60	2.66	23.26	1.90

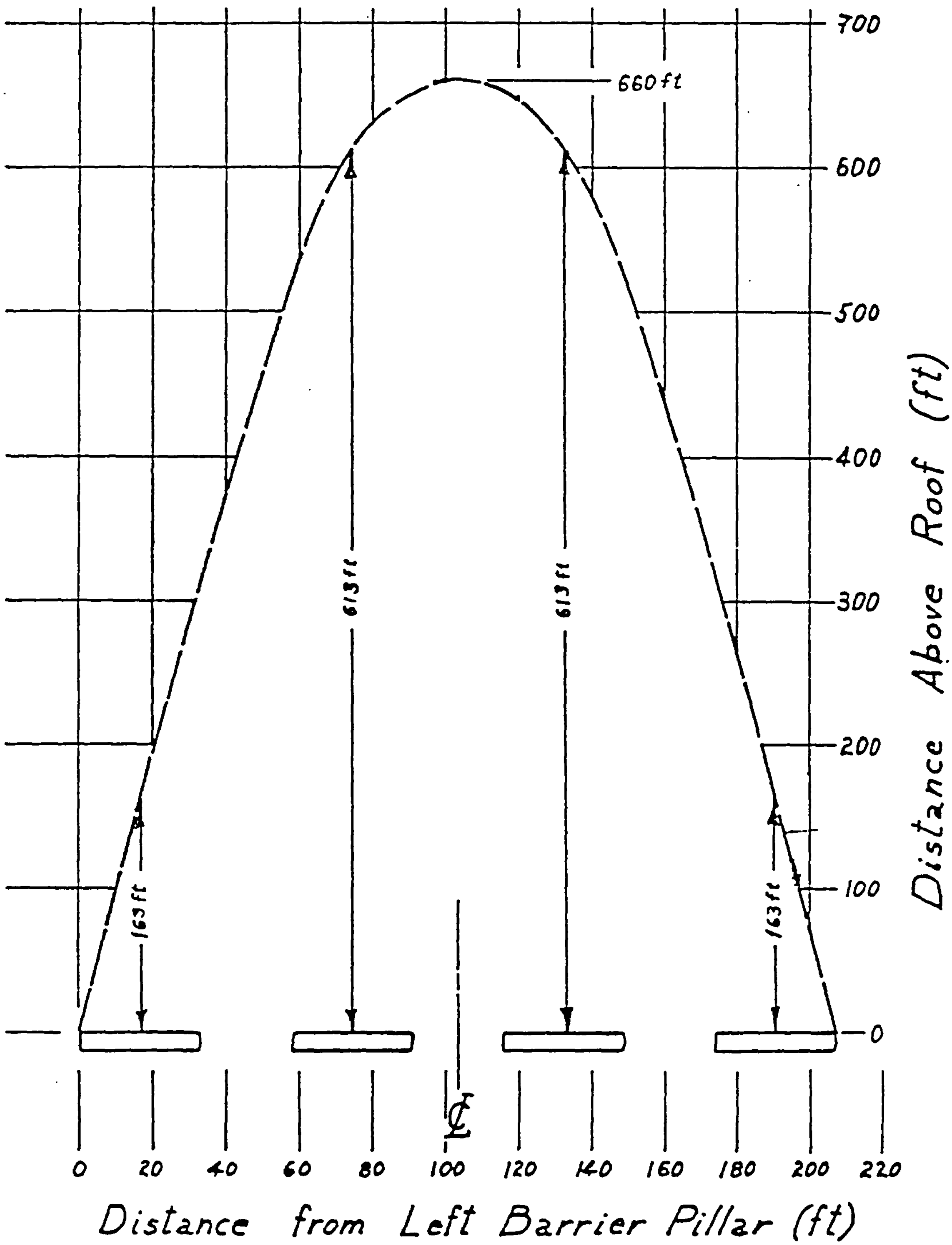

Predicted arch load on room yield pillars.

Figure 11.

undergo creep deformation. Figure 12 presents the Lomenick creep equation predicted abutment pillar shortening as well as the yield load induced shortening of the QUAD room pillars. The storage room pillars will undergo repeated cycles of yielding as the abutment pillars yield more rapidly than the much more lightly loaded room pillars. This is not the case for the entry pillars because of the greater than load transfer distance of unmined adjacent salt, and thereby their isolation from the influence of nearby excavation.

The Lomenick creep equation predicted pillar shortening for the rigid abutment pillar in QUAD Design #1. Lomenick's specimen creep equation probably underestimates the magnitude of pillar shortening, because of the size/strength relationship. However, the relative magnitudes of pillar shortening should occur, irrespective of what creep equation is employed.

I recommend that the abutment pillars be enlarged to 400-ft in width in order to better isolate sets of storage rooms from each other.

SHOP PILLARS

Two shop pillars were evaluated for their ability to function as rigid pillars within the overall shaft pillar. They are extreme northwest shop pillar (#1) which has a 28.2-ft high side on the south and 12-ft high sides on the other three sides. The other pillar checked (#2) is directly east of the first pillar and is 12-ft high on all sides. Shop pillar #1 is approximately 220 by 150 ft and the area it is assumed to support is 286 by 175 ft. Shop pillar #2 is approximately 226 by 120 ft and its tributary area is assumed to be 286 by 145 ft. No load carrying capability was assumed for the 20-ft wide pillars at the north and south ends of both pillars. Table 7 indicates predicted factors of safety of nearly 2.0 as rigid pillars. These compare favorably with the overall shaft pillar safety factors. The other shop pillars appear to be equally strong or stronger.

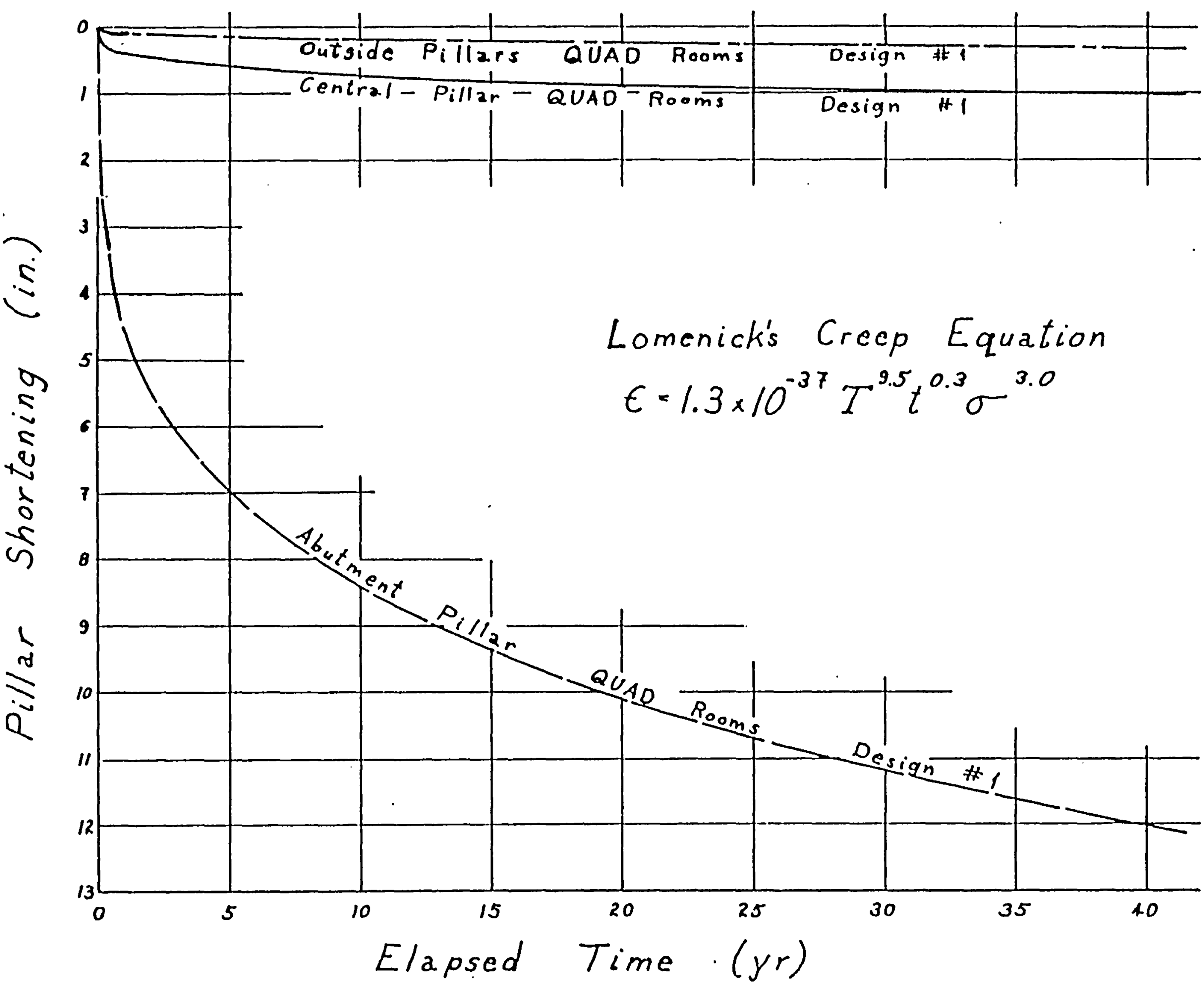
Outside Pillars QUAD Rooms Design #1
Central - Pillar - QUAD Rooms Design #1
Lomenick's Creep Equation
$\epsilon = 1.3 \times 10^{-37} T^{9.5} t^{0.3} \sigma^{3.0}$
Abutment Pillar QUAD Rooms Design #1
Pillar Shortening (in.)
Elapsed Time (yr)
0
1
2
3
4
5
6
7
8
9
10
11
12
13
0
5
10
15
20
25
30
35
40

Figure 12a.

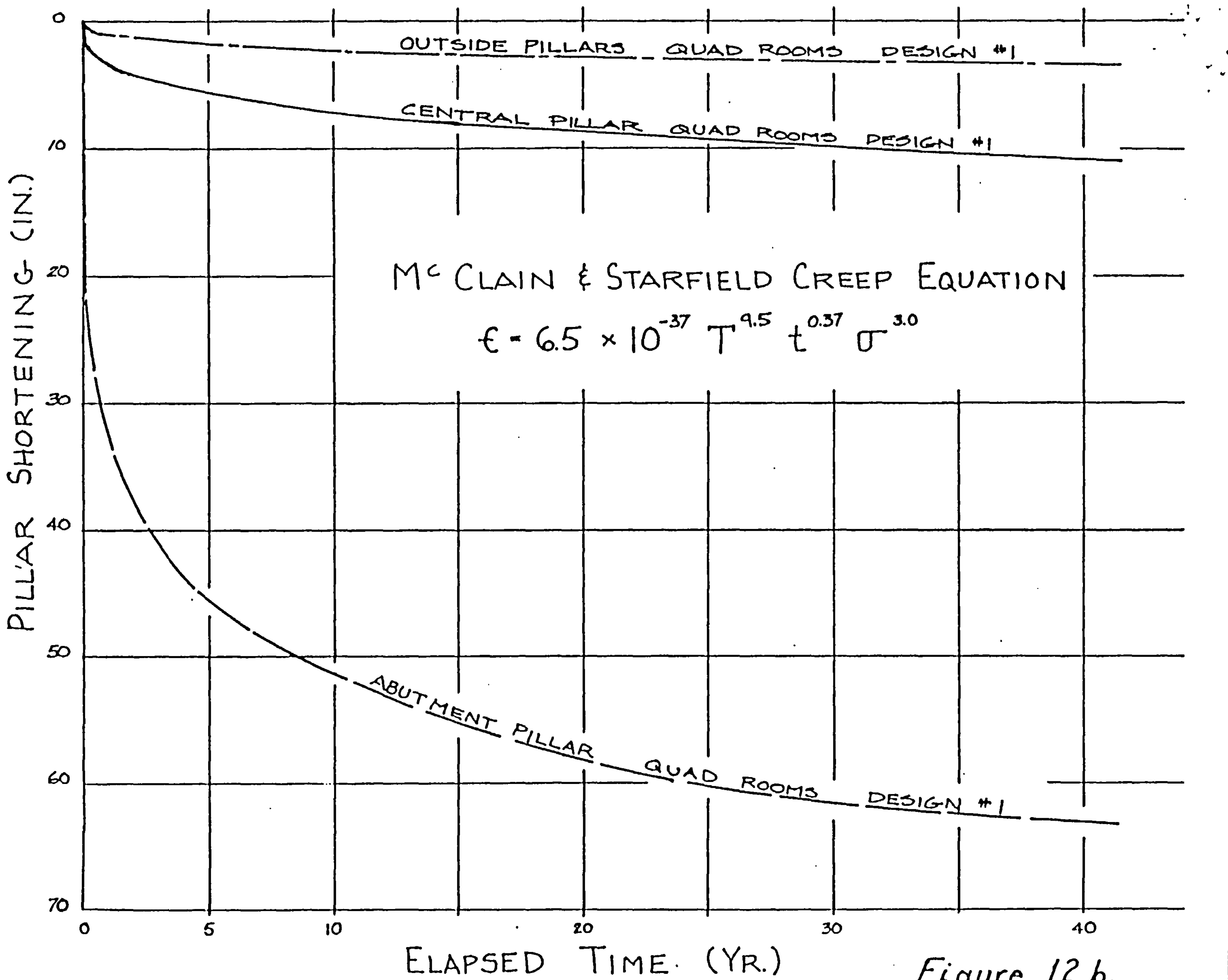
OUTSIDE PILLARS QUAD ROOMS DESIGN #1
CENTRAL PILLAR QUAD ROOMS DESIGN #1
ABUTMENT PILLAR QUAD ROOMS DESIGN #1
M^c CLAIN & STARFIELD CREEP EQUATION
$\epsilon = 6.5 \times 10^{-37} T^{9.5} t^{0.37} \sigma^{3.0}$
PILLAR SHORTENING (IN.)
ELAPSED TIME (YR.)
0
10
20
30
40
50
60
70
0
5
10
20
30
40

Figure 12 b.

TABLE 7

FACTORS OF SAFETY FOR
SHOP PILLARS #1 AND #2

PILLAR	TAL (tons x 10^6)	STRENGTH $\phi = 30^o$; σ_o = 450psi (tons x 10^6)	FS	STRENGTH $\phi = 30^o$; σ_o = 937psi	FS
#1	7.49	13.86	1.85	15.38	1.98
#2	6.21	11.55	2.05	12.78	2.06

SHAFT PILLAR RADIUS

Shaft pillar design has been a critical problem for as long as shaft mining has been undertaken. Twenty-one shaft pillar design formula have been extracted from the mining literature. The value of these empirical shaft pillar design equations lies in the warning they would sound if the WIPP design were to fall outside conventional practice. The range of shaft pillar radii predicted for the WIPP conditions by the twenty applicable empirical design formula is from 100 ft to 1200 ft. The mean predicted shaft pillar radius is 485 ft. The WIPP shaft pillar design radius of 1000 ft falls at the conservative end of the range.

The design of the shaft and shaft pillar is normally the most conservative part of mine design. Two prime considerations control the selection of a radius for the "life-of-the-mine" shaft pillar. These are strength and subsidence.

The factor of safety (FS) for the proposed 1000-ft radius shaft pillar was first calculated. The tributary area load applied was the weight of all the rock above and one load transfer distance outward from the 1000-ft radius shaft pillar. Initially, no reduction was made for any transfer of load to pillars outside the shaft pillar and all these pillars were assumed to have failed. Figure 13 presents a section through such a pillar. The factor of safety for $\Phi = 30^{\circ}$ and σ_{o} = 450 psi is <u>1.65</u> and for $\Phi = 30^{\circ}$ and σ_{o} = 937 psi is <u>1.77</u>. Next, the rock under the arch was assumed to load onto the pillars outside the shaft. This increases the factor of safety to <u>2.43</u> and <u>2.62</u> for the respective physical properties.

The radius of shaft pillar necessary to carry the maximum tributary area load <u>FS = 1</u>, (radius plus transfer distance) was then calculated. The resulting radii are 500 ft for $\Phi = 30^{\circ}$ and σ_{o} = 450 psi and 460 ft for $\Phi = 30^{\circ}$ and

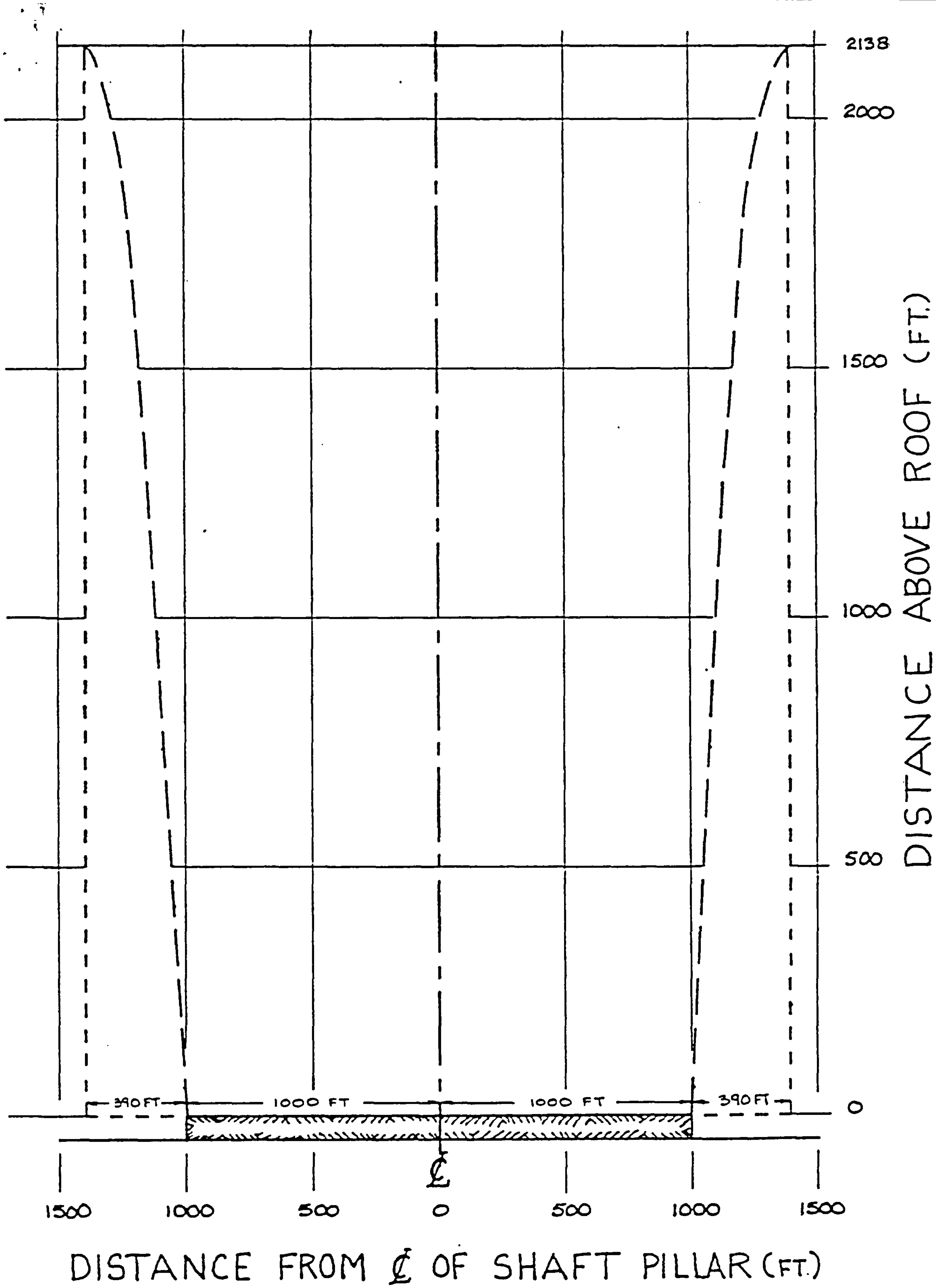

2138
2000
1500
1000
500
0
DISTANCE ABOVE ROOF (FT.)
390 FT
1000 FT
1000 FT
390 FT
℄
1500
1000
500
0
500
1000
1500
DISTANCE FROM ℄ OF SHAFT PILLAR (FT.)

Figure 13

σ_o = 937 psi. When the rock under the arch is transfered to the pillars the factor of safety rises to <u>1.96</u> for $\phi = 30^0$ and σ_o = 450 psi and to <u>2.12</u> for $\phi = 30^0$ and σ_o = 937 psi.

Subsidence shaft pillar design criteria are related to the subsidence tolerance of structures that are placed above the shaft pillar. Table 8 presents strain and tilt limits indicated as acceptable by the references listed. The British National Coal Board (NCB) damage prediction versus length of structure is presented on Figure 14 and the relative effects on Table 9.

The calculation of surface subsidence effects using the NCB Subsidence Engineers Handbook predicts maximum tensile strain over the ribside of 1070 $\mu\epsilon$ for Design #1. These are noticeable strains but tolerable for most surface structures. The resulting strain at the shaft collar is 214 $\mu\epsilon$ for Design #1 for a 1000-ft radius shaft pillar and storage rooms placed right up against the shaft pillar. Figure 15a shows the most adverse shaft pillar configuration for horizontal strain development.

TABLE 8: Acceptable subsidence effects

Horizontal Strain (μϵ)	Vertical Strain (μϵ)	Tilt (α) Tan α	α (')	Comments and References
1000	1000	0.0010	3.43'	"tolerable level of strain likely to be on the order of"---for shaft (1)
1500	1500	0.0025	8.58'	Polish Category I (2)
3000	3000	0.0050	17.18'	Polish Category II (2)
6000	6000	0.0100	34.36'	Polish Category III (2)
9000	9000	0.0150	51.57'	Polish Category IV (2)
500 to 1000	500 to 1000			High continuous brick walls (3)
1000 to 2000	1000 to 2000			One-story brick mill (3) building, wall cracking
1000	1000			Plaster cracking (gypsum) (3)
2500 to 4000	2500 to 4000			Reinforced-concrete (3) building frame
3000	3000			Reinforced-concrete (3) curtain walls
5000	5000			Steel frame, (3) continuous simple steel frame
		0.004	13.75'	Tilting of smoke-stacks (3) towers
		0.010	34.37'	Rolling of trucks, (3) stacking of goods

TABLE 8:

(continued)

Horizontal Strain ($\mu\epsilon$)	Vertical Strain ($\mu\epsilon$)	Tilt (α) Tan α	α (')	Comments and References
				Machine operations: (3)
		0.003	10.32'	Cotton loom
		0.0002	0.68'	turbo-generator
		0.003	10.32'	Crane rails (3)
		0.01 to 0.02	34.37' to 68.75'	Floor drainage (3)

References from Bibliography

(1) Wagner & Salamon, 1973

(2) Salamon, 1964

(3) Voight & Pariseau, 1970

TABLE 2. - Categories of protection, Poland

Category	Allowable tilt, x 10^{-3}	Allowable strain, x 10^{-3}	Explanation
I	2.5	1.5	Allowable are slight damage such as hair cracks in plaster.
II	5.0	3.0	Allowable are small reparable damage .
III	10.0	6.0	Allowable are damage that do not destroy the building or impair its service.
IV	15.0	9.0	Movements are such that completely reinforced structures are required to resist them.

Figure 14

Relationship of Damage to Length of Structures and Horizontal Ground Strain

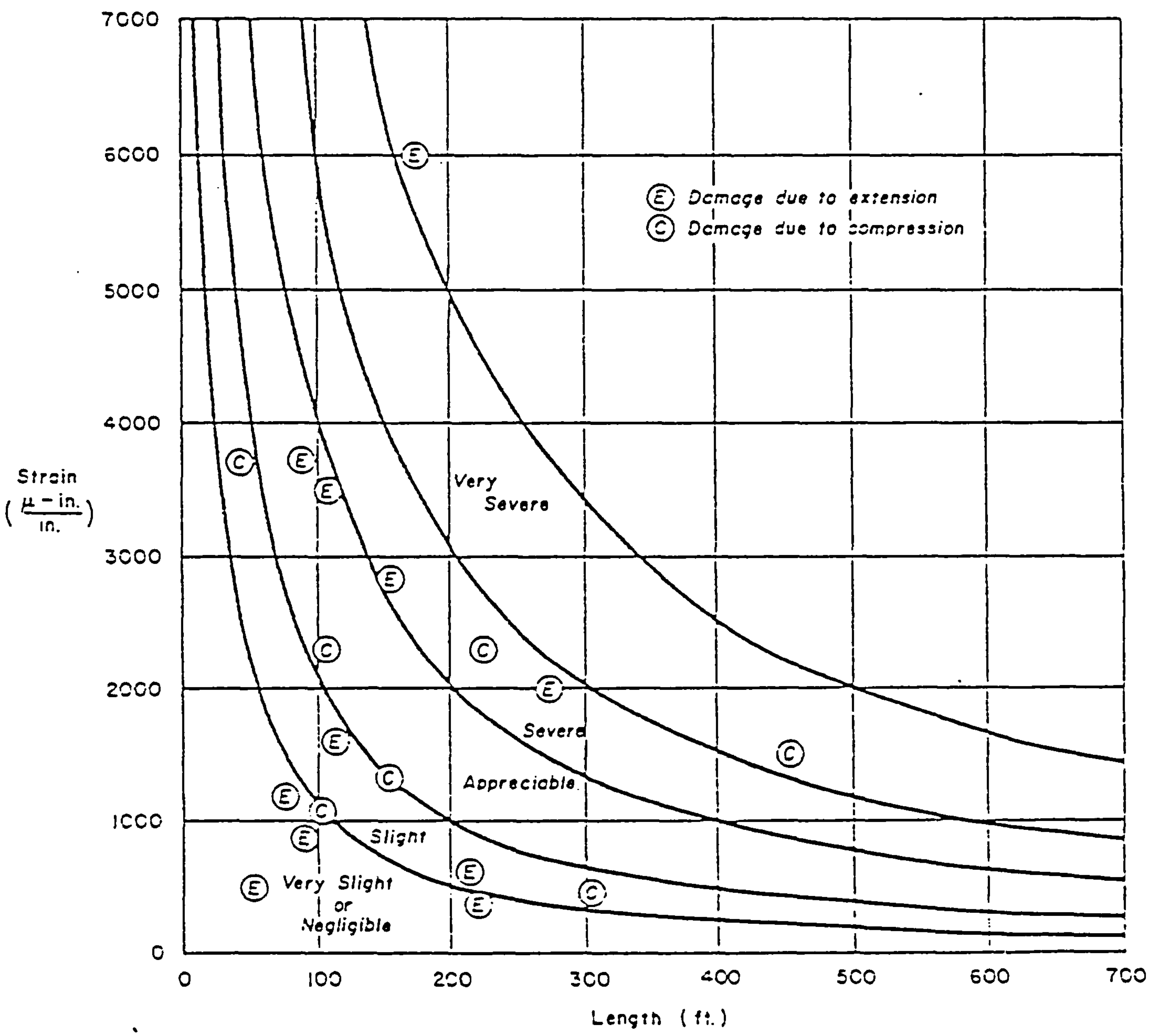

TABLE 9 - SUBSIDENCE DAMAGE DESCRIPTION FOR HORIZONTAL STRAIN

Class of damage	Change of length of structure	Description of typical damage
Very slight or negligible Example: 50-ft long building extended	Up to 0.1 ft	Hair cracks in plaster. Perhaps isolated slight fracture in the building, not visible on outside. 50 u - in./in.
Slight Example: 110-ft long building extended	0.1 ft-0.2 ft	Several slight fractures showing inside the building. Doors and windows may stick slightly. Repairs to decoration probably necessary. 1,600 u - in./in.
Appreciable Example: 90 ft long building extended	0.2 ft-0.4 ft	Slight fractures showing on outside of building (or one main fracture). Doors and windows sticking; service pipes may fracture. 3,700 u - in./in.
Severe Example: 220 ft long apartment house under compression	0.4 ft-0.6 ft	Service pipes disrupted. Open fractures requiring rebonding and allowing weather into the structure. Window and door frames distorted; floors sloping noticeably. Some loss of bearing in beams. If compressive damage, overlapping of roof joints and lifting of brickwork with open horizontal fractures. 2,300 u - in./in.
Very severe Example: 180 ft long apartment house with extension of	More than 0.6 ft	As above, but worse, and requiring partial or complete rebuilding. Roof and floor beams lose bearing and walls lean badly and need shoring up. Windows broken with distortion. Severe slopes on floors. If compressive damage, severe buckling and bulging of the roofs and walls. 6,000 u - in./in.

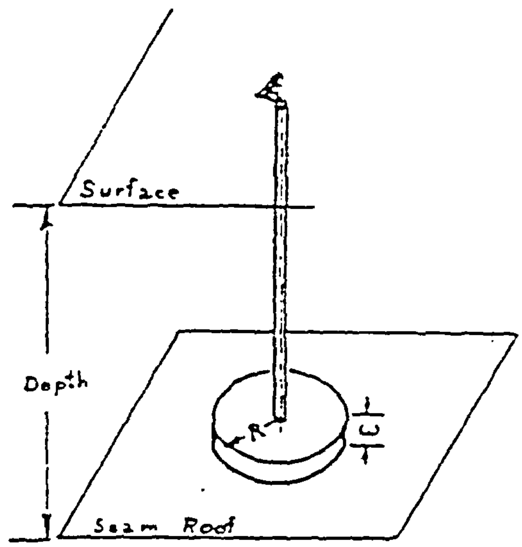

(a) Most Adverse Pillar Configuration for Horizontal Strain Development

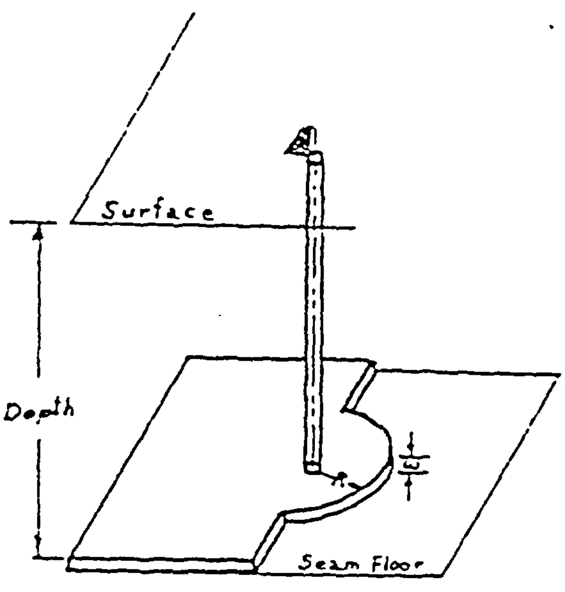

(b) Most Adverse Pillar Configuration for Development of Tilt

(adapted from Daemen, 1972 and Wagner & Salamon, 1973)

Figure 15

DESIGN VERIFICATION TEST

The early verification of yield pillar design is imperative. The entries in the shop area will provide any early opportunity to test and instrument single entries, 20- by 28.2-ft near the construction and exhaust shaft, 26- by 12-ft near the ventilation and supply and service shaft and 25- by 12-ft on the west and east sides of the shop area. In addition, the 20- by 12-ft and 12- by 12-ft entries to the early development area will provide further testing for single openings.

The test panel for Design #1 QUAD rooms is too short to provide a meaningful test of the yield pillars. At the time these rooms are driven there will be effectively infinite pillars at their northern and southern ends. These test yield pillars will only approximate the majority of planned yield pillars in the actual storage area. Figures 11 and 16 indicate the predicted east-west and north-south yield pillar rock arch loads over the test panel. The configuration shown would have to be lengthened considerably to subject a meaningful length of the test yield pillars to the actual storage room conditions. In addition, the abutment pillars adjacent to the test rooms will not be loaded to the same degree as planned storage rooms. Consideration should be given to a set of yield pillar rooms to the east of the test panel, since the shortening of the abutment pillar is predicted to exceed the shortening of the yield pillars. This latter problem with the test panel can probably be accounted for by careful calculation.

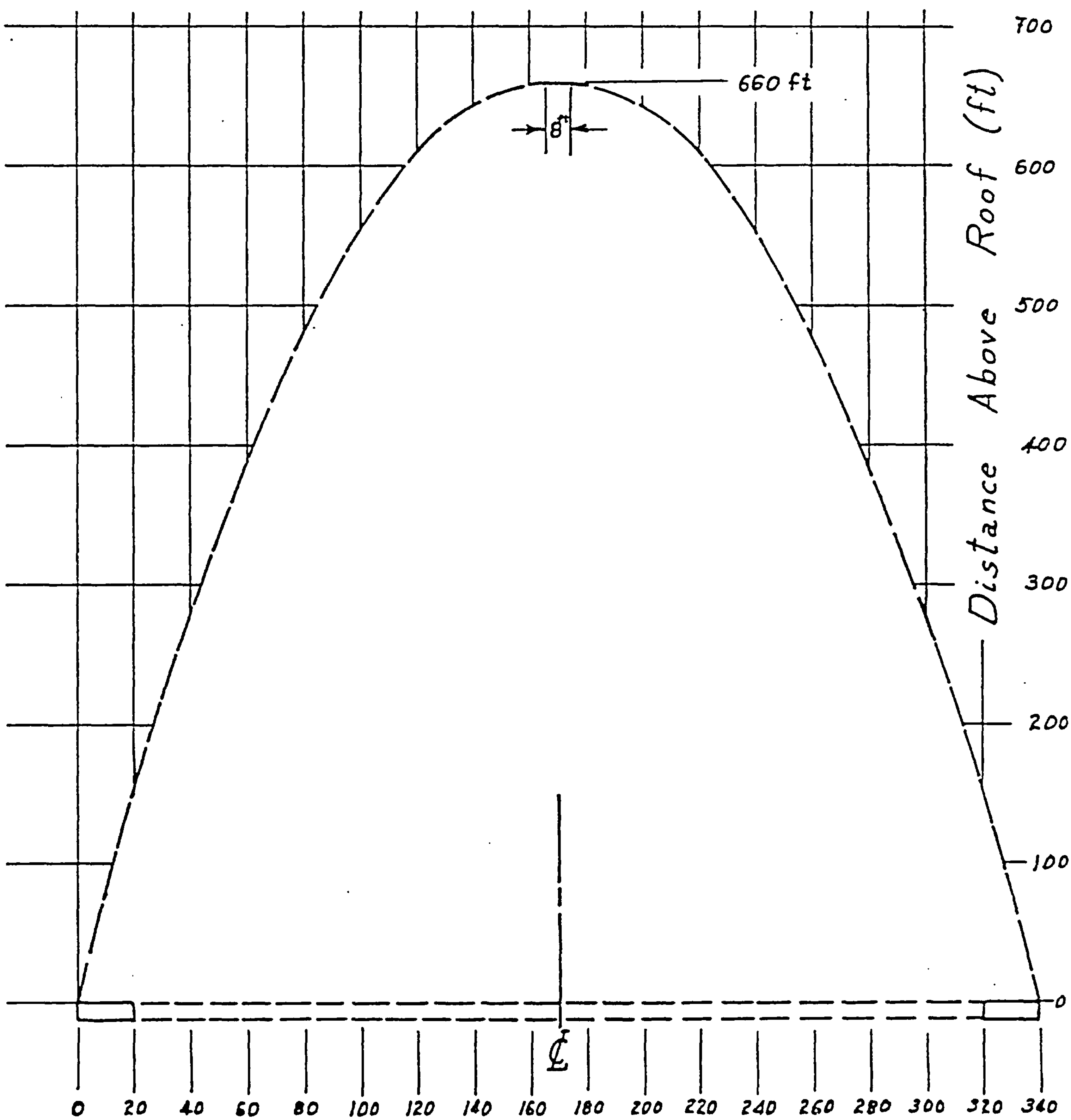

Distance from Left Barrier Pillar (ft)

Predicted arch load N-S on central test pillar.

Figure 16

REVIEW OF CREEP CONSTANTS

The potential variability in creep rates in bedded salt mines was indicated by the data presented by Hedley (1967, p. 122) and presented graphically on Figure 17. Table 10 presents creep constants reported in the literature. It is unfortunate that their is so much difference indicated in these constants.

An effort was made to fit the 5 in. of reported vertical closure over a 3 year period at the Kerr-McGee Mine near Carlsbad, NM (p. 7 of Sept. 13, 1979 trip report). The initial conditions given were 25-ft width rooms, 100-ft pillars and approximately 1900-ft depth. The assumed room height was varied, using 7-ft, 6-ft and 5-ft. These heights are based on a visit by the author to the mine in 1974. The measured and predicted room closures are presented on Table 11. The predicted room closures have been corrected by including the effect of decreasing pillar stress with increasing pillar width. Rock temperature was assumed a constant 27^{o} C.

The apparently better prediction of vertical room closure with the McClain and Starfield (1977) equation is probably the result of its being produced from actual field data. The Lomenick (1968) creep equation was developed from model tests in the laboratory. The size/strength relationship for rocks, previously discussed, no doubt accounts for major parts of the difference between these equations.

EVALUATION OF ROOF MEMBER

The indicated thickness of salt without clay partings above the roof of the storage rooms is 15 ft. Such a thickness of roof eliminates the possibility of tensile bending failure at the center of the roof. In addition, the minor increase in compressive bending stress at the roof beam ends over the ribsides

Figure 17: Convergence rates measured in salt mines (Data from Hedley, 1967)

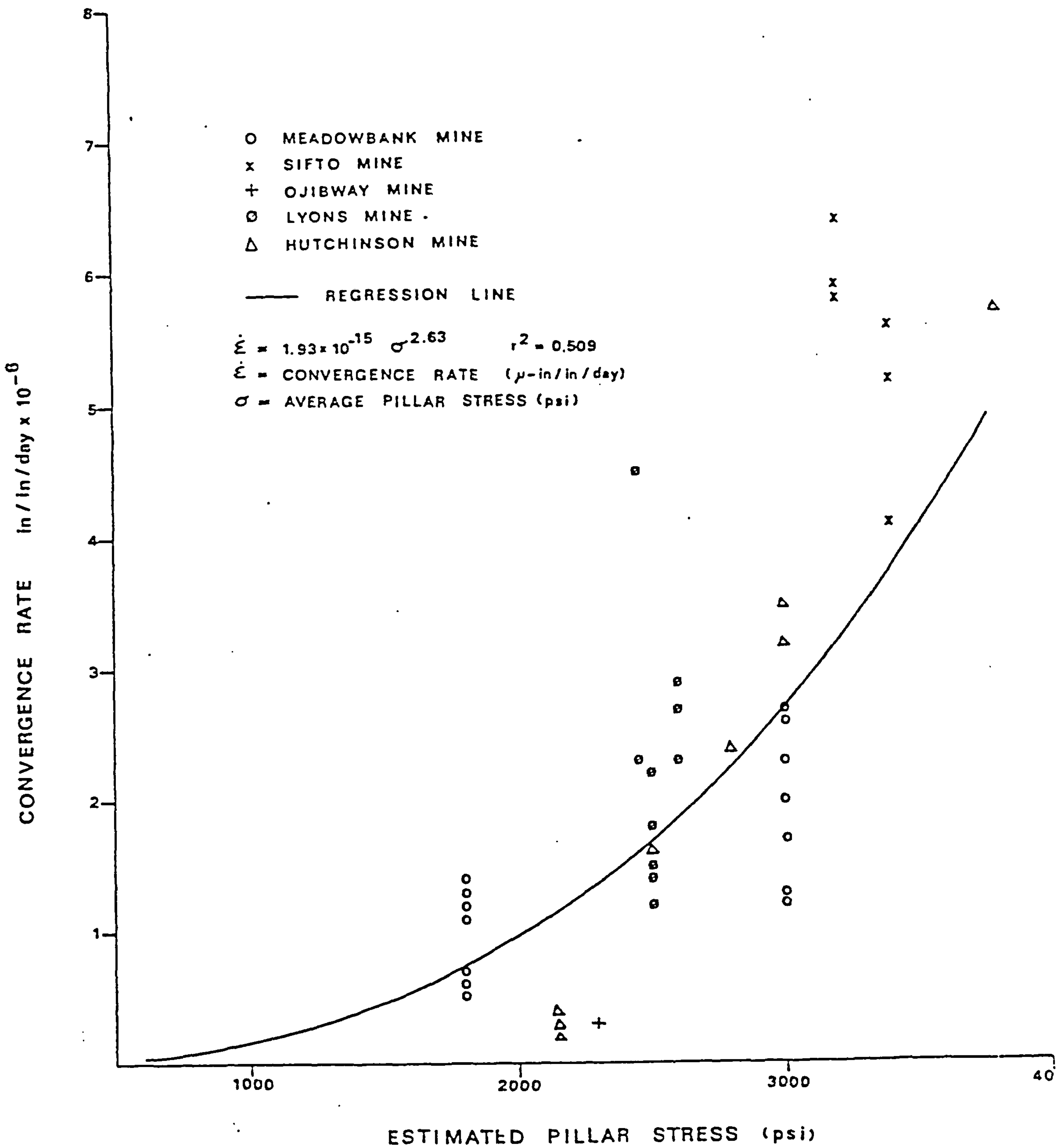

TABLE 10

CREEP CONSTANTS FROM LITERATURE

Reference	Linear Constant	Stress Exponent	Time Exponent	Temperature Exponent
Obert (1964)		3.0		
Bradshaw (1964)		3.1	0.4	
Hedley (1967)		2.7 (2.63)*		
Lomenich (1968)	1.3×10^{-37}	3.0	0.3	9.5
Starfield & McClain (1973)	0.65×10^{-37}	3.0	0.25	9.5
McClain & Starfield (1977)	6.5×10^{-37}	3.0	0.37	9.5
Hardy & St. John (1977)	0.65×10^{-36}	3.0	0.4	9.5

* Exponent calculated by power curve fit of Headley's data in 4th Canadian Rock Mechanics Symposium

TABLE 11

MEASURED AND PREDICTED VERTICAL
CLOSURE (Kerr-McGee Mine, Carlsbad, MN)

Reference & Equation	Initial Room Height(in.)	Vertical Closure After 3 Years Measured (in.)	Predicted (in.)	Percent of Measured
Lomenick (1968)	84	5	0.78	16%
$\epsilon = 1.3 \times 10^{-37} \ T^{9.5} \ t^{0.3} \ 3.0$				
McClain & Starfield (1977)	84	5	8.31	166%
	72	5	7.75	155%
	60	5	5.94	119%
$\epsilon = 6.5 \times 10^{-37} \ T^{9.5} \ t^{0.32} \ 3.0$				

should not prouce a compressional roof failure at those locations. The following beam analysis presents the pertinent calculations

GIVEN: $\gamma = 140$ lb/ft^3; $\sigma_{ovb} = \sigma_{hor} = 2080$ psi

$\ell = 33$ ft; $h = 15$ ft

$$\sigma = \sigma_{hor} \pm \sigma_f; \quad \sigma_f = \frac{Mc}{I}; \quad c = h/2$$

$$I = \frac{bh^3}{12}; \quad M_{end} = \frac{w\ell^2}{12}; \quad M_{cen} = \frac{w\ell^2}{24}$$

CALCULATION:

$$c = 15/2 = 7.5 \text{ ft}$$

$$I = \frac{(1)\ (15)^3}{12} = 281 \text{ ft}^4; \quad w = 15\ (140) = 2100 \text{ lb/ft}$$

$$M_{end} = \frac{2100\ (33)^2}{12} = 191{,}000 \text{ ft-lb}$$

$$\sigma_{end} = 2080 + \frac{191000\ (7.5)}{281\ (144)} = 2080 + 40 = \underline{\underline{2120 \text{ psi}}}$$

$$\sigma_{cen} = 2080 - 20 = \underline{\underline{2060 \text{ psi}}}$$

Because of the indicated stability of the roof, brittle failure, in the unlikely event of such a failure, should occur as hourglassing of the ribsides of the abutment pillar facing the storage rooms.

HORIZONTAL CANISTER PLACEMENT

Placement of RH canisters in horizontal 40-in. diameter holes drilled into the ribs of the abutment pillars may reactivate their creep sequence. If these 40-in. diameter holes are drilled 17.2 ft into the rib at 8-ft centers approximately 5400 ft^2 of pillar area will removed from the abutment pillar per side. It appears unlikely that canisters will be placed into the storage room sides of the abutment pillars because of the high stress at those locations and the possibility of CH waste storage in the adjacent rooms. The stress increase resulting from 8-ft center horizontal canister storage on the two access drift sides of the abutment pillars will be approximately 13.6%. The stress increase for 10-ft center canister placement is approximately 8.0%

The reactivation of the abutment pillar creep just before retreat from the access drift will decrease the time between placement and encapsulation by the backfilled salt.

CONCLUSIONS

Despite the predicted stability of the yield pillar design I can see no compelling reason to use it. The WIPP design is in no way related to maximizing extraction under adverse geologic conditions. The selection of the storage horizon was made to provide a thick stable roof member and pillars free of ~~day~~ CLAY partings.

The yield pillar entries and storage pillars should be stable, even after horizontal holes are drilled some 17 ft from each access drift into the storage room abutment pillars. There is no apparent reason not to use abutment pillars of dimensions that exceed the load transfer distance.

The shop pillars appear fully capable of carrying tributary area loads.

The shaft pillar radius appears to be rather conservative. Exactly how conservative depends on the strain and tilt tolerance of planned surface structures.

The design verification yield pillar test panel should be extended at least 100 ft in the north-south direction in order to subject the central 100 or so ft of the yield pillars to approximately the same loading as the storage room yield pillars. Otherwise, the yield pillar loads will be less than in their storage area locations.

REFERENCES

Abel, J.F., Jr., 1961, Ice tunnel closure phenomena: U.S. Army Snow, Ice & Perafrost Res. Est. Tech. Rpt. 74, 37 p.

Abel, J.F., Jr., and Hoskins, W.N., 1976, Confined core pillar design for Colorado oil shale: Proc. 9th Symp. on Oil Shale, Quant. Colo. School of Mines, vol. 71, no. 4, pp. 287-308.

Baar, C.A., 1965, Measurements of rock pressure and pillar loads in deep potash mines: Proc. 2nd Symp. on Salt, vol. 2, p. 18-23.

Baar, C.A., 1972, Creep measured in deep potash mines vs. theoretical predictions: 7th Canadian Rock Mech. Symp., pp. 23-77.

Baar, C.A., 1977, Applied salt-rock mechanics 1, Elsevier, 294 p.

Bradshaw, R.L., Boegly, W.J., and Empson, F.M., 1964, Correlation of convergence measurements in salt mines with laboratory creep test data: Proc. 6th U.S. Symp. on Rock Mech., pp. 501-514.

Brauner, G., 1973, Subsidence due to underground mining (in two parts), Part 1. Theory and practices in predicting surface deformation: U.S. Bureau of Mines I.C. 8571, 56 p., Part 2. Ground movements and mining damage: U.S. Bureau of Mines I.C. 8572, 53 p.

Dravo, Corp., 1974, Analysis of large scale non-coal underground mining methods: U.S. Bureau of Mines contract S0122059, N.T.I.S. Number PB 234 555, 605 p.

Hardy, M.P., and St. John, C.M., 1977, Surface displacements and pillar stresses associated with nuclear waste disposal in salt: Proc. 18th U.S. Symp. on Rock Mech., pp. 4B7-1 - 4B7-6.

Hedley, D.G.F., 1967, An appraisal of convergence measurements in salt mines: Proc. 4th Canadian Rock Mech. Symp. pp.

Hedley, D.G.F., 1972, An evaluation of roof stability at a Canadian salt mine: Proc. 5th Int'l. Strata Control Conf., Paper 30, 6 p.

Hofer, K.H., and Menzel, W., 1964, Comparative study of pillar loads in potash mines established by calculation and by measurements below ground: Int'l Jour. Rock Mech. and Min. Sci., vol. 1, no. 2, pp. 181-198.

Lomenick, T.F., 1968, Accelerated deformation of rock salt at elevated temperature and pressure and its implication for high level radioactive waste disposal: Ph.D. Dissertation, Univ. of Tenn., (ORNL-TM-2102).

McClain, W.C. and Starfield, A.M., 1977, Analysis of combined effects in Project Salt Vault: Demonstration of the disposal of high-activity solidified wastes in underground salt mines, Bradshaw and McClain, eds., Chap. 13, ORNL-4555 UC-70.

McClain, W.C., 1964, Time dependent behavior of pillars in the Alsace potash mines: Proc. 6th U.S. Symp. on Rock Mech., pp. 489-500.

Menzel, W., Eckart, D., Bruckner, G., and Thoma, K., 1972, Pillar and room dimensioning methods in potash mining, as developed by the Mines Safety Institute in Leipzig: Proc. 5th Int'l Strata Control Conf., Paper 27, 9 p.

Metcalf, J.R., 1966, Angle of repose and internal friction: Int'l. Jour. Rock Mech. and Min. Sci., vol. 3, no. 2, pp. 155-161.

Miller, E.H., and Pierson, F.L., 1958, Underground movement and subsidence over United States Potash Company mine: Preprint 5819P9, Soc. Mining Engrs. of AIME.

National Coal Board, 1975, Subsidence engineers handbook: London NCB, 111 p.

Obert, L., 1965, Creep in model pillars: U.S. Bureau of Mines, Rpt. of Inv. 6703, 23 p.

Potts, E.L.J., Potts, W.H., and Szeki, A., 1972, The development of ground control techniques and mining design parameters in rock salt mining: Proc. 5th Int'l. Strata Control Conf., Paper 21.

Reynolds, T.D., and Gloyna, E.F., 1961, Creep measurements in salt mines: Proc. 4th U.S. Symp. on Rock Mech., pp. 11-17.

Seldenrath, I.T.R., 1954, Coal measure rocks considered as elastic and loose material and the load on props on an advancing face: Leeds Univ. Min. Soc. Jour., vol. 30, pp. 39-49.

Serata, S., 1972, The Serata stress control method of stabilizing underground openings: Proc. 7th Canadian Rock Mechanics Symp., pp. 99-118.

*Starfield, A.M., and McClain, W.C., 1973, Project Salt Vault: a case study in rock mechanics: Int'l Jour. Rock Mech. and Min. Sci. and Geomech. Abstracts, vol. 10, no. 6, pp. 641-657.

Steart, F.A., 1954, Strength and stability of pillars in coal mines: Chem., Met., and Min. Soc. S. Africa Jour., vol. 54, pp. 309-325, 392-399.

Voight, B., and Pariseau, W., 1970, State of predictive art in subsidence engineering Jour. Soil Mech. and Found. Div. ASCE, vol. 96, SM2, pp. 721-749.

Wagner, H., and Salamon, M.D.G., 1972, Strata control techniques in shafts and large excavations: Assoc. Mine Mgrs. S. Africa, Papers and Disc., vol. 1972-73, pp. 123-140.

Wilson, A.H., 1972, Research into the determination of pillar size, PartI. An hypothesis concerning pillar stability: The Mine Engr., vol. 131, no. 141, pp. 409-417.

APPENDIX A

CONFINED CORE PILLAR LOADING ANALYSIS

Adapted from: A.H. Wilson, Research into the determination of pillar size, Part I, An hypothesis concerning pillar stability, The Mining Engineer, v. 131, n. 141, pp. 409-417, June 1972.

Terminology Employed

p = Pillar width (ft) ; ℓ = Pillar length (ft)
m = Pillar height (ft) ; H = Depth (ft)
γ = Density (lb/ft^3) ; ϕ = Angle of internal friction ($^\circ$)
$Tan\,\beta$ = $1 + \sin\phi / 1 - \sin\phi$ (Passive pressure coefficient)
σ_o = Compression strength (psi) at pillar ribside. (Rock substance cohesion is a conservative estimate.)
σ_V = Vertical stress at seam level (psi)

$\widehat{\sigma_V}$ = Maximum stable vertical pillar stress (psi).

Y = Distance into pillar (ft)
$\hat{Y}$ = Distance into pillar at location of maximum stable pillar stress (ft), or to edge of confined core.
L = Load carrying capacity of pillar (Tons).
σ_B = Average bolting stress applied to pillar edge (psi).

σ_F = Fill stress applied horizontally at midheight of pillar (psi).
ϕ_F = Angle of repose (surface friction) of fill ($^\circ$)
γ_F = Density of fill (lb/ft^3)

$$\sigma_F = \frac{m\gamma_F}{2}\left(\frac{1 - \sin\phi_F}{1 + \sin\phi_F}\right) \quad \text{psi}$$

$$\widehat{\sigma_V} = (6.944 \times 10^{-3}\,\gamma H + \sigma_F)\,Tan\,\beta + \sigma_o \quad \text{psi}$$

$$\widehat{\sigma_V} \simeq 4(1.1\,H) + \sigma_o$$

$$\hat{Y} = \frac{m}{\sqrt{Tan\,\beta}\,(Tan\,\beta - 1)}\ln\frac{\widehat{\sigma_V}}{\sigma_o + (\sigma_F + \sigma_B)Tan\,\beta} \quad \text{ft}$$

Figure

Passive pressure potential for confined
central core of a pillar

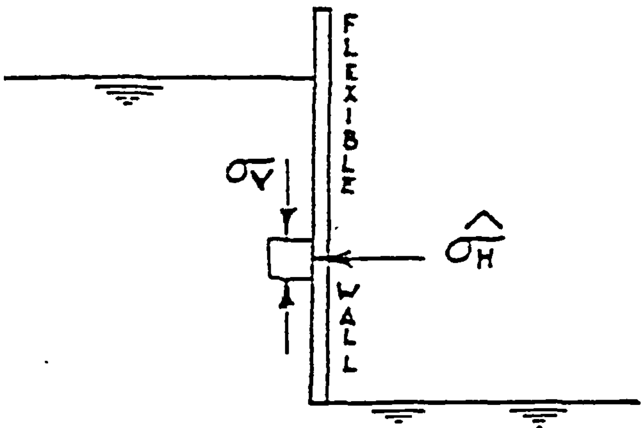

$$\text{Passive } \hat{\sigma}_H = \left(\frac{1 + \sin \Phi}{1 - \sin \Phi}\right)\sigma_V + C$$

Φ = Angle of internal friction

C = Soil cohesion

σ_V = Overburden (confining) stress

$\hat{\sigma}_H$ = Stress necessary to push aside soil confined by "σ_V" and with cohesion of "C" (Passive resistance of soil)

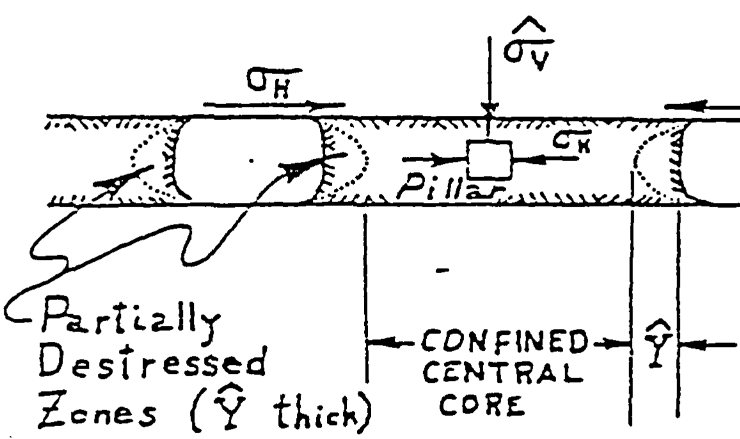

$$\text{Passive } \hat{\sigma}_V = \left(\frac{1 + \sin \Phi}{1 - \sin \Phi}\right)\sigma_H + \sigma_o$$

σ_H = Horizontal (confining) stre

σ_o = Rock mass uniaxial compression strength

$\hat{\sigma}_V$ = Maximum stable vertical pillar stress under confinement of "σ_H" and with rock mass uniaxial compression strength "σ_o".

WIDE PILLARS $2\hat{Y} < P$

(a) Square Pillars

$$L = 7.2 \times 10^{-2} \widehat{\sigma_v} \left[P^2 - 2P\hat{Y} + \frac{4}{3}\hat{Y}^2 \right] \text{Tons}$$

(b) Rectangular Pillars

$$L = 7.2 \times 10^{-2} \widehat{\sigma_v} \left[P\ell - P\hat{Y} - \ell\hat{Y} + \frac{4}{3}\hat{Y}^2 \right] \text{Tons}$$

(c) Circular Pillars

$$L = 5.655 \times 10^{-2} \widehat{\sigma_v} \left[P^2 - 2P\hat{Y} + \frac{4}{3}\hat{Y}^2 \right] \quad \text{Tons} \qquad p = \text{diameter}$$

(d) Long Pillars

$$L = 7.2 \times 10^{-2} \widehat{\sigma_v} \left[P - \hat{Y} \right] \quad \text{Tons per foot of run}$$

NARROW PILLARS $2\hat{Y} > P$ potentially unstable

(a) Square Pillars

$$L = 7.2 \times 10^{-2} \widehat{\sigma_v} \left[\frac{P^3}{6\hat{Y}} \right] \quad \text{Tons}$$

(b) Rectangular Pillars

$$L = 7.2 \times 10^{-2} \widehat{\sigma_v} \left[\frac{P^2}{2\hat{Y}} \left(\frac{\ell}{2} - \frac{P}{6} \right) \right] \quad \text{Tons}$$

(c) Circular Pillars

$$L = 0.009425 \widehat{\sigma_v} \left[\frac{P^3}{\hat{Y}} \right] \quad \text{Tons} \qquad p = \text{diameter}$$

(d) Long Pillars

$$L = 7.2 \times 10^{-2} \widehat{\sigma_v} \left[\frac{P^2}{4\hat{Y}} \right] \quad \text{Tons per foot of run}$$

IRREGULAR SHAPED PILLARS
(Straight sides-Wide Pillars)

(a) Potential tons of load on core per ft^2

$$L = (5.0 \times 10^{-4} \gamma H + \sigma_B) \text{ OR } L = 7.2 \times 10^{-2} \widehat{\sigma_v} \quad \text{tons per } ft^2$$

(b) Potential tons of load per running foot of exposed pillar Wall

$$L = (6.94 \times 10^{-3} \gamma H + \sigma_B)\, \hat{Y}/2 \tan\beta \text{ Tons per foot of run}$$

$$\text{OR} \quad L = 7.2 \times 10^{-2} \quad \hat{Y}/2 \left[\widehat{\sigma_v} \right]$$

WIDE PILLAR

$\hat{Y} < P/2$

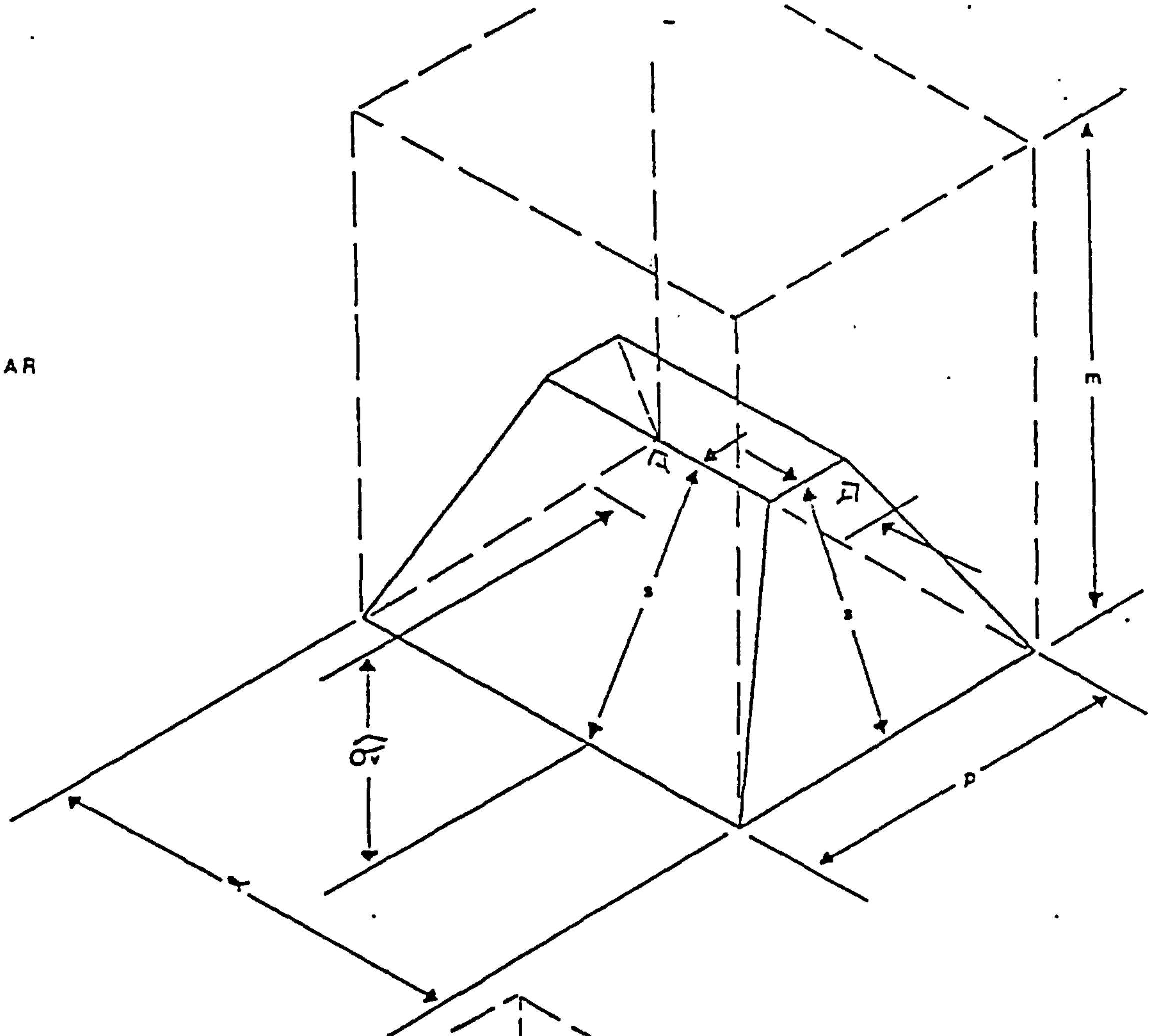

NARROW PILLAR

$\hat{Y} > P/2$

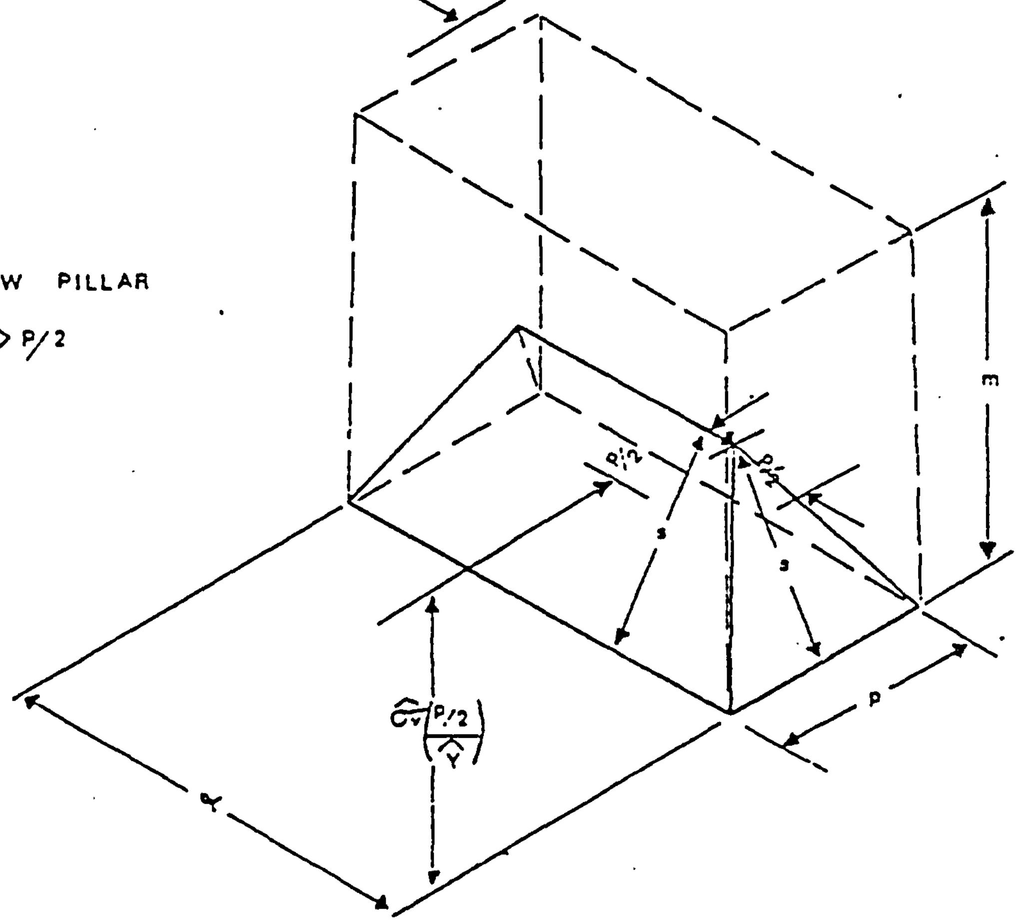

FIGURE LOAD-CARRYING CAPACITY, OR MAXIMUM STRESS, DISTRIBUTION DIAGRAM

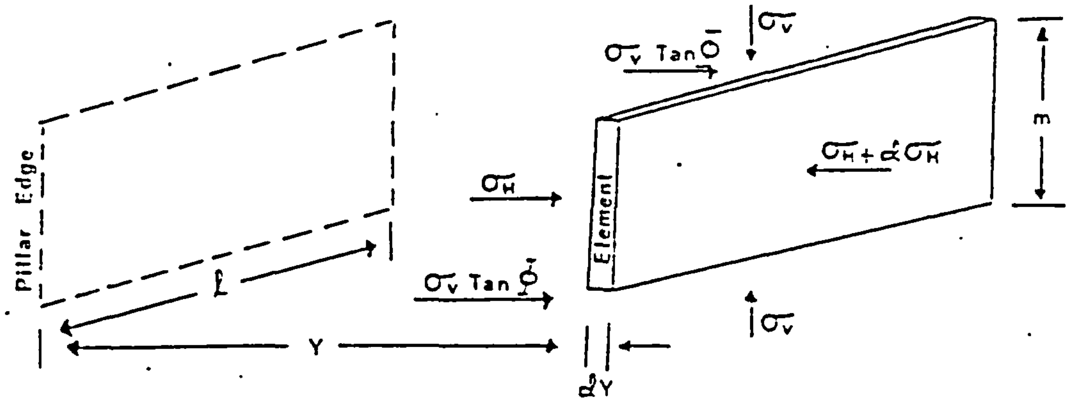

PURPOSE: FIND DEPTH INTO PILLAR TO PEAK (MAXIMUM) STABLE VERTICAL PILLAR STRESS

(1) Force tending to move element is

$$(\sigma_H + d\sigma_H)m\ell - \sigma_H m\ell = d\sigma_H m\ell = m\ell\, d\sigma_H$$

(2) Frictional resistance top plus bottom

$$2\sigma_V \,\text{Tan}\,\bar{\phi}\,\ell\, dY$$

(3) Stability requires

$$m\ell\, d\sigma_H = 2\sigma_V \,\text{Tan}\,\bar{\phi}\,\ell\, dY$$

$$m\, d\sigma_H = 2\sigma_V \,\text{Tan}\,\bar{\phi}\, dY$$

$$d\sigma_H = \frac{2\sigma_V \,\text{Tan}\,\bar{\phi}\, dY}{m}$$

(4) Confined strength

$$\sigma_V = \sigma_0 + \text{Tan}\,B\,\sigma_H$$

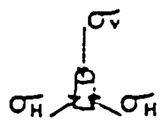

(5) Increment of stress (vertical) increase across element

from (3) $d\sigma_V = \text{Tan}\,B\, d\sigma_H$ Constant σ_0 lost during differentiation

$$d\sigma_V = \text{Tan}\,B\left(\frac{2\sigma_V \,\text{Tan}\,\bar{\phi}\, dY}{m}\right)$$

$$\frac{d\sigma_V}{dY} = \frac{2\,\text{Tan}\,B\;\text{Tan}\,\bar{\phi}\,\sigma_V}{m} \qquad \frac{dY}{d\sigma_V} = \frac{m}{2\,\text{Tan}\,B\;\text{Tan}\,\bar{\phi}}\left(\frac{1}{\sigma_V}\right)$$

(6) Passive Pressure Equivalents

$$\text{Tan}\,B = \frac{1 + \text{Sin}\,\bar{\phi}}{1 - \text{Sin}\,\bar{\phi}} \qquad \text{Tan}\,\bar{\phi} = \frac{\text{Tan}\,B - 1}{2\sqrt{\text{Tan}\,B}}$$

from (5)

$$\frac{dY}{d\sigma_V} = \frac{m}{2\,\text{Tan}\,B\left(\dfrac{\text{Tan}\,B - 1}{2\sqrt{\text{Tan}\,B}}\right)}\left(\frac{1}{\sigma_V}\right)$$

$$\frac{dY}{d\sigma_V} = \frac{m\sqrt{\text{Tan}\,B}}{\text{Tan}\,B\,(\text{Tan}\,B - 1)}\left(\frac{1}{\sigma_V}\right) = \frac{m}{\sqrt{\text{Tan}\,B}\,(\text{Tan}\,B - 1)}\left(\frac{1}{\sigma_V}\right)$$

$$dY = \frac{m}{\sqrt{\text{Tan}\,B\,(\text{Tan}\,B - 1)}}\left(\frac{1}{\sigma_V}\right)d\sigma_V$$

(7) Distance ($\hat{Y}$) into pillar to location of Maximum vertical stable pillar stress ($\hat{\sigma_v}$)

$$\int_0^{\hat{Y}} dY = \frac{m}{\sqrt{\tan\delta\,(\tan\delta - 1)}} \int_{\sigma_0}^{\hat{\sigma_v}} \frac{1}{\sigma_v}\, d\sigma_v$$

$$\hat{Y} = \frac{m}{\sqrt{\tan\delta}\,(\tan\delta - 1)} \ln \frac{\hat{\sigma_v}}{\sigma_0}$$

APPENDIX B

CALCULATION OF SHOP PILLAR STABILITY

Pillar # 1 - Northeast

LOADING (TAL)

$$\text{Tributary Area} = (220 + 26 + 20 + 10 + 10)(150 + 25)$$
$$= (286)(175) = 50050 \text{ ft}^2$$

$$\text{Tributary Area Load} = (50050)(2138)(140)/2000$$
$$= 7.49 \times 10^6 \text{ Tons}$$

STRENGTH

$$(\phi = 30^0;\ \sigma_o = 450 \text{ psi})$$

Pillar height (m) = 12 ft (3 Sides)

= 28.2 ft (South Side)

Maximum Stable Vertical Stress ($\hat{\sigma}_v$)

$$v = \sigma_o + H\ Tan\beta$$

$$an\beta = \frac{1 + Sin\Phi}{1 - Sin\Phi} = 3.0$$

$$\hat{\sigma}_v = 450 + 2138\left(\frac{140}{144}\right)3.0 = 6686 \text{ psi}$$

Thickness of Yield Zone ($\hat{Y}$)

$$\hat{Y} = \frac{m}{\sqrt{Tan\beta}\,(Tan\beta - 1)}\ \ln\frac{\hat{\sigma}_v}{\sigma_o}$$

$$m = 12 \text{ ft}$$

$$\hat{Y} = \frac{12}{\sqrt{3}\,(3-1)}\ \ln\frac{6686}{450} = 9.348 \text{ ft}$$

$$m = 28.2$$

$$\hat{Y} = \frac{28.2}{\sqrt{3}\,(3-1)}\ \ln\frac{6686}{450} = 21.968 \text{ ft}$$

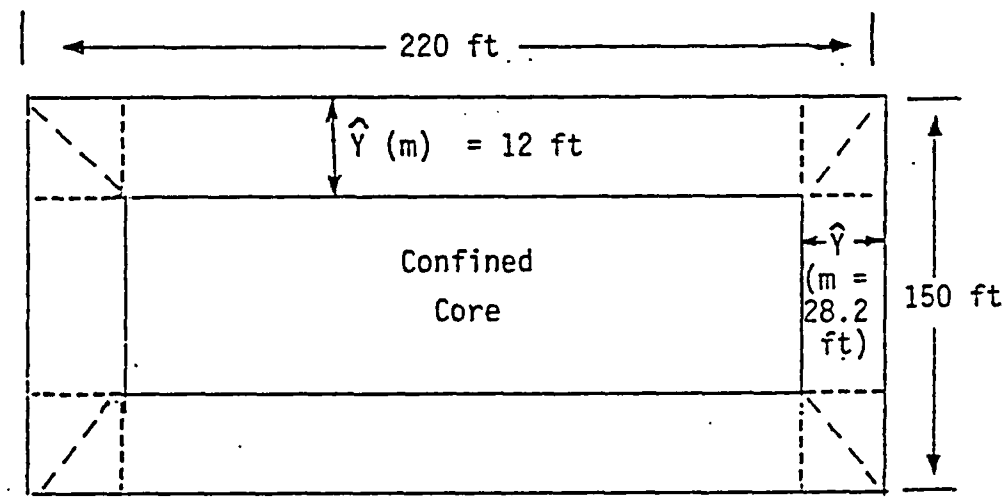

Confined Core Area

$$(220 - 9.348 - 21.968)\left[150 - 2\,(9.348)\right] = 24780\ \text{ft}^2$$

Confined Core Strength

$$\frac{(24780)\,(144)\,(6686)}{2000} = 11.93 \times 10^6\ \text{Tons}$$

Ribside Length (m = 12 ft)

$$2\,(220 - 9.348 - 21.968) + \left[150 - 2\,(9.348)\right]$$
$$2\,(188.684) + (131.304) = 508.7\ \text{ft}$$

Ribside Strength (m = 12 ft)

$$\frac{508.7\,(6686)\,(9.348)\,(144)}{2\,(2000)} = 1.14 \times 10^6\ \text{Tons}$$

Ribside Strength (m = 28.2)

$$\frac{\left[150 - 2\,(9.348)\right]\,(6686)\,(21.968)\,(144)}{2\,(2000)} = 0.69 \times 10^6\ \text{Tons}$$

Corner Strength (m = 12 ft)

$$2\left[1/3\ \frac{(9.348)^2\,(6686)\,(144)}{2000}\right] = 0.03 \times 10^6\ \text{Tons}$$

Corner Strength (m = 12 ft and 28.2 ft)

$$2\left[1/3\ \frac{(9.348)\ (21.968)\ (6686)\ (144)}{2000}\right] = 0.07 \times 10^{6} \text{ Tons}$$

<u>CUMMULATIVE STRENGTH</u> (L)

$$= 13.86 \times 10^{6} \text{ Tons}$$

FACTOR OF SAFETY

$$FS = \frac{L}{TAL} = \frac{13.86 \times 10^{6}}{7.49 \times 10^{6}} = \underline{\underline{1.85}}$$

APPENDIX C

SHAFT PILLAR DESIGN FORMULAS

All dimensions converted to ft from original yds, fathoms and ft.

S = Side length recommended for square shaft pillar.

D = Diameter recommended for circular shaft pillar.

R = Radius recommended for circular shaft pillar.

H = Depth

t = Seam thickness extracted or in the case of back filling the effective seam thickness extracted.

Merivale (Colliery Engr., 1897, p. 538) Side length of square shaft pillar equal to 66 times the square root of the depth in ft. divided by 300

$$S = 66\sqrt{\frac{H}{300}}$$

South African (Daemen, 1972) Shaft pillar radius equal to 10% of the depth.

$$R = 0.1H$$

Andre (Colliery Engr., 1897, p. 538) Side length of square shaft pillar is 105 ft to a depth of 450 ft, with 1-ft additional for each 5-ft of additional depth.

$$S = 105 + \frac{H-450}{5}$$

Indiana (Parsons, 1910) - Side length of square shaft pillar equal to the sum of 1% of the depth (ft) plus 5 ft all multiplied by the thickness of the seam extracted in ft.

$$S = t(0.01H + 5)$$

Wardle (Colliery Engr., 1897, p. 538) Side length of square shaft pillar is 120 ft to a depth of 360 ft, with 1-ft additional for each 4-ft of additional depth.

$$S = 120 + \frac{H-360}{4}$$

Strahan (Coal Miner's Pocket Book, 1928) Angle of draw outside surface area to be protected ranges from 15° for "thin seams" to 8° for "thick seams".

$$H \operatorname{Tan} 8^\circ \leqslant R \leqslant H \operatorname{Tan} 15^\circ$$

$$2H \operatorname{Tan} 8^\circ \leqslant S \leqslant 2H \operatorname{Tan} 15^\circ$$

Pamely (1891) - Side length of square shaft pillar 40 yds to a depth of 100 yds, plus 1 yd in length for each additional 4 yds of depth.

$$S = 120 + \frac{H-300}{4}$$

Central Coal Basin, IL (Young & Stoek, 1916) Leave 100 square feet of coal for each foot of depth.

$$S = \sqrt{100H}$$

$$R = \sqrt{\frac{100H}{\pi}}$$

Dron (Colliery Engr., 1897, p. 538) Side length of square shaft pillar equal to 1/3 the depth to protect surface.

$$S = \frac{H}{3}$$

Scottish (Young & Stoek, 1916) Leave 1/3 to 1/5 larger pillar than surface area to be protected, i.e. an of angle of draw from 1/6 to 1/10 (9.5° tp 5.7°)

$$\frac{H}{10} \leqslant R \leqslant \frac{H}{6}$$

$$\frac{H}{5} \leqslant S \leqslant \frac{H}{3}$$

Dickinson (Hughes, 1904) Radius for hard coal measures (Lancashire) and seams not exceeding 6-ft in thickness:

$$R = \frac{H}{10} + \frac{H}{10} = 0.20H$$

Radius for medium strata:

$$R = \frac{H}{7.5} + \frac{H}{10} = 0.23H$$

Radius for soft strata:

$$R = \frac{H}{5} + \frac{H}{10} = 0.30H$$

Silesian (Redmayne, 1914) - Angle of draw outside the surface area to be protected is 12^{o}, decreasing with depth.

$$R = H \tan 12^{o}$$

$$S = 2H \tan 12^{o}$$

O'Donahue (Mason, 1951) The radius of the shaft pillar on the rise side equal to $M + \frac{H}{7} + \frac{2Y}{3}$, on the dip side $M + \frac{H}{7} - \frac{Y}{3}$ and along strike $M + \frac{H}{7}$

M = Margin of safety equal to 5 to 10% of the depth

$Y = H\sin\alpha \cos\alpha$

α = angle of dip

Flat bedded (Assumes angle of draw = 8^{o})

$$0.19H \leqslant R \leqslant 0.24H$$

Northumberland/Durham - (Boulton, 1908) Radius equal 1/4 the depth

$$R = \frac{H}{4}$$

Mining Engrg. (London) (Colliery Engr., 1897, p. 117)
Radius of 60 ft plus 1/10 the depth multiplied by the square root of 1/3 the effective seam thickness extracted.

$$R = 60 + \frac{H}{10}\sqrt{\frac{t}{3}}$$

Strahan (1956) - Diameter of circular shaft pillar in a flat seam will usually be 2/3 of the depth of the seam.

$$D = \frac{2H}{3}$$

$$R = \frac{H}{3}$$

Foster (Colliery Engr., 1897, p. 538) Radius of circular shaft pillar equal to three times the square root of the product of the depth times the thickness of seam extracted.

$$R = 3\sqrt{Ht}$$

Boulton (1908) - Radius equal to 1/6 the depth plus twice the square root of the product of depth and seam thickness.

$$R = \frac{H}{6} + 2\sqrt{Ht}$$

Mason (1951) Radius of circular shaft pillar equal to between 1/4 and 1/2 the depth, or side length of square shaft pillar equal to between 1/2 and full depth.

$$\frac{H}{4} \leqslant R \leqslant \frac{H}{2}$$

$$\frac{H}{2} \leqslant S \leqslant H$$

Longden (Hughes, 1904) Radius of shaft pillar equal to 1/2 the depth.

$$R = \frac{H}{2}$$

Stewart (Colliery Engr., 1897, p. 189) In South Wales minimum radius of pillar from shaft 450-ft for 600-ft depth plus 1-ft for each 2-ft additional depth to 1500-ft depth. Remains constant at 900-ft radius below 1500-ft depth.

$$R = 450 + \frac{H-600}{2}$$